Magnetic monopole becomes dyon in topological insulators

Shoto Aoki, Hidenori Fukaya, Naoto Kan, Mikito Koshino, and Yoshiyuki Matsuki
Department of Physics, Osaka University, Toyonaka, Osaka 560-0043, Japan

(Received 10 May 2023; accepted 30 August 2023; published 3 October 2023)

The Witten effect predicts that a magnetic monopole acquires a fractional electric charge inside topological insulators. In this work, we give a microscopic description of this phenomenon as well as an analogous two-dimensional system with a vortex. We solve the Dirac equation of electron field both analytically in a continuum and numerically on a lattice by adding the Wilson term and smearing the gauge field within a finite range to regularize the short-distance behavior of the system. Our results reveal that the Wilson term induces a strong positive mass shift, creating a domain-wall around the monopole or vortex. This small yet finite-sized domain wall localizes the chiral zero modes and ensures their stability through the Atiyah-Singer index theorem, whose cobordism invariance is crucial in explaining why the electric charge is fractional.

DOI: 10.1103/PhysRevB.108.155104

I. INTRODUCTION

The magnetic monopole has been a fascinating object in particle physics. It explains the quantized nature of electric charges of elementary particles [1], describes duality of the Maxwell theory under exchange of electric and magnetic fields, and appears as a stable solitonic state in grand unified theories [2,3]. Although it has not been discovered yet, even its absence plays a role in supporting the inflation scenario of the early universe, where the density of the monopoles became extremely small [4].

In this article our focus is on one of remarkable theoretical predictions about a monopole: that it gains a nonzero electric charge in the so-called θ vacuum with a nonzero angle. This prediction arises from a direct coupling between electric and magnetic fields and is known as the Witten effect [5]. The effect has provided significant insights into understandings of quantum field theory and string theory [6–13].

Nontrivial θ dependence can appear from a nonzero expectation value of the axion field background, which has been actively discussed in various studies [14–20]. However, our universe is essentially in the $\theta = 0$ vacuum, where the CP symmetry with C transformation (exchanging electrons and positrons) and P transformation (exchanging left-handed and right-handed spins) is manifestly maintained.[1] The only known exception is topological insulators [21–26], which effectively induce the vacuum angle $\theta = \pi$, and the CP and time-reversal (T) symmetries are protected in a nontrivial way.

Then an interdisciplinary question between particle and condensed-matter physics arises: what will happen to a magnetic monopole when it is put inside a topological insulator? According to the prediction in Ref. [5], it will become a dyon with a half-integral electric charge. A macroscopic understanding of the Witten effect in condensed-matter physics was reported in Refs. [24,27,28]. In this work, we aim to provide a microscopic understanding of the mechanism behind the capture of the electric charge by the monopole. While it is difficult to identify the origin of the electric charge from the θ term added in the Maxwell theory, it is almost obvious that the electron is the only candidate in condensed matter. Then we should address the following issues: (1) how a monopole can capture an electron state, (2) why this phenomenon does not occur in normal insulators, and (3) why the charge is not an integer but a half integer.

In this study, we solve the Dirac equation in the presence of a monopole both analytically in continuum and numerically on a lattice. Additionally, we investigate a vortex in a two-dimensional topological insulator, which also captures a half-integral charge [29–31], and we find that the microscopic mechanism of the electron capture is the same for both cases. To distinguish between normal and topological insulators and to eliminate UV divergence near the monopole or vortex, we introduce the Wilson term in the Dirac operator. We also smear the magnetic charge and flux distribution in a range of finite radius r_1 to study the origin of the nontrivial boundary condition [32] at the singularity of the gauge fields. Our computation is UV finite everywhere, allowing us to safely take the $r_1 \to 0$ limit without any ambiguity.

Our study reveals dynamical formation of a domain wall around the monopole or vortex with a finite radius. Inside the domain wall, the electron enters the trivial phase due to an additive mass shift caused by the dense magnetic field in the Wilson term. This means that the neighborhood of the monopole or vortex becomes a normal insulator island. In contrast with the standard argument where the electron zero mode is captured by the zero-dimensional defect of the gauge field [33–40], the bound state can be identified as a chiral edge mode [41–45] on the codimension-one domain wall around the monopole or vortex. The chiral boundary condition arises as a dynamical consequence of the domain-wall formation rather than an artificial boundary condition imposed by hand.

[1] In this work we ignore a tiny CP violation coming from the weak interaction.

We find that the chiral modes near the monopole or vortex obey a massless Dirac equation on the domain-wall where a strong curvature induces a gravitational connection [46–48]. This gravitational effect leads to a gap in the Dirac Hamiltonian, which is counteracted in our system by the magnetic field of the monopole or vortex resulting in the zero eigenvalue. Moreover, we demonstrate that the chiral zero modes are topologically linked via the Atiyah-Singer (AS) index [49,50] (or mod-two AS index [51] for the vortex) to the total magnetic flux inside the domain wall. Thus, the existence of the zero modes is topologically protected.

The cobordism invariance of the AS index requires the existence of an additional zero mode localized at the surface of the topological insulator with the opposite chirality, which is also topologically protected. This has been empirically observed in previous numerical studies [39,40,48,52]. The paired two zero modes must mix while maintaining the $\pm$ symmetry of the Dirac Hamiltonian spectrum. Since only one of the two (near) zero modes is occupied in the half-filling state, and only half of its amplitude is located near the monopole or vortex, the zero-mode mixing naturally explains the half integral electric charge in the vicinity of the monopole or vortex.

Furthermore, the creation of the domain wall offers an intriguing reinterpretation of the conventional θ vacuum approach in the Maxwell theory. The defect in the θ term does not necessarily require a point-like magnetic charge. If we could introduce a thin solenoid with a sufficiently dense magnetic flux into a topological insulator, we might be able to verify experimentally that the magnetic "monopole-like" configuration captures half of an electric charge. In this study, we simulate this system on a lattice by gradually increasing the magnetic flux of the solenoid. We find that the charge is pumped not from the bulk but from the outer surface of the topological insulator, where the Dirac string becomes a bridge between the two domain walls. In contrast to the standard bulk-edge correspondence [53,54] of the chiral anomaly, our system exhibits the "edge-edge" correspondence of the zero modes.

The rest of the paper is organized as follows: In Sec. II, we review the original semiclassical effective theory approach with the θ term and Chern-Simons term in the Maxwell theory in three and two dimensions, respectively. Our analysis starts from a vortex in a two-dimensional topological insulator in Sec. III and continues to our main target: a monopole in a three-dimensional topological insulator in Sec. IV. In Sec. V, we numerically confirm pairing of the zero modes: one located at the monopole and the other at the surface of the topological insulator. Then we try to reinterpret the original effective theory approach in Sec. VI, simulating a solenoid whose end produces essentially the same phenomenon as the Witten effect. In Sec. VII, we give a summary and discussion.

II. EFFECTIVE THEORY DESCRIPTION OF MONOPOLE OR VORTEX GAINING ELECTRIC CHARGES

First we review the standard understanding how the monopole becomes a dyon when the effective theory contains the $\theta \neq 0$ term. Let us consider a Dirac fermion determinant with a mass m in four dimensions regularized by a Pauli-Villars (PV) field[2] with a mass M_{PV},

$$Z = \det\left(\frac{D+m}{D+M_{\mathrm{PV}}}\right), \tag{1}$$

where $D = \gamma^\mu D_\mu = \gamma^\mu(\partial_\mu + iA_\mu)$ is the Dirac operator with the U(1) electro-magnetic gauge field A_μ. Here we take M_{PV} positive and $m < 0$ in a T-symmetry-protected topological insulator.

When we perform an axial U(1) rotation to flip the mass sign, the anomaly produces the $\theta = \pi$ term,

$$Z = \det\left(\frac{D+|m|}{D+M_{\mathrm{PV}}}\right)e^{iS_{\mathrm{top.}}}, \tag{2}$$

where the topological action $S_{\mathrm{top.}}$ is

$$S_{\mathrm{top.}} = \pi\frac{1}{32\pi^2}\int d^4x F_{\mu\nu}\tilde{F}^{\mu\nu}, \tag{3}$$

where $F_{\mu\nu}$ is the field strength of the U(1) gauge field, and $\tilde{F}^{\mu\nu} = \epsilon^{\mu\nu\rho\sigma}F_{\rho\sigma}$ with the antisymmetric Levi-Civita tensor $\epsilon^{\mu\nu\rho\sigma}$. Reducing the cutoff $M_{\mathrm{PV}} \to |m|$, or equivalently integrating out the fermions, the remaining effective action is the $\theta = \pi$ term.

The θ term modifies the Maxwell equation in the vacuum to

$$\partial_\mu F^{\mu\nu} = -\frac{\theta}{8\pi^2}\partial_\mu\tilde{F}^{\mu\nu}. \tag{4}$$

The $\nu = 0$ component relates the divergence of the electric field $\boldsymbol{E}$ to that of the magnetic field $\boldsymbol{B}$. The Gauss law around the monopole is then

$$q_e = \int d^3x \nabla\cdot\boldsymbol{E} = -\frac{\theta}{4\pi^2}\int d^3x \nabla\cdot\boldsymbol{B} = -\frac{\theta q_m}{\pi}. \tag{5}$$

When the magnetic charge q_m is nonzero, the electric charge q_e is also nonzero. In particular, when the monopole has a unit magnetic charge $q_m = 1/2$ (in terms of the Dirac's quantization condition), the electric charge[3] at $\theta = \pi$ is $-1/2$.

In a similar way, the $(2+1)$-dimensional effective action of a single Dirac fermion in a topological phase is the Chern-Simons action with level $k = 1$, which modifies the Maxwell equation to

$$\partial_\mu F^{\mu\nu} = -\frac{k}{8\pi^2}\epsilon^{\nu\rho\sigma}F_{\rho\sigma}, \tag{6}$$

and the vortex with flux α gains an electric charge through the Gauss law

$$q_e = \int d^2x \nabla\cdot\boldsymbol{E} = -\frac{k}{2\pi}\int d^2x\epsilon^{0\rho\sigma}F_{\rho\sigma} = -k\alpha. \tag{7}$$

When $\alpha = 1/2$ and k is odd, the electric charge is fractional.

This effective theory description is quite simple but cannot answer the following questions: (1) What is the origin of electric charge? (2) If the origin is the electron field, why is

[2]To fully regularize the theory, we need multiple PV fields. However, for the tree-level computation in this work, one bosonic spinor field is enough.

[3]From the 2π periodicity of θ, $-1/2$ mod $\mathbb{Z}$ is allowed.

it bounded to a monopole or vortex? (3) Why is the electric charge fractional? In the following sections, we try to answer these questions, revealing the microscopic features of the electron field in the presence of the monopole or vortex.

III. TWO-DIMENSIONAL VORTEX

We start our analysis from a two-dimensional massive Dirac fermion, which represents a model of electron fields in a two-dimensional topological insulator. As will be shown below, the microscopic mechanism explaining how a vortex gains an electric charge is essentially the same as what happens on a monopole in a three-dimensional topological insulator. Summary of analytic results and some numerical analysis on a lattice were already presented in Refs. [47,48] by two of the authors.

A. A naive Dirac equation

First we review the standard analysis of the Dirac equation in the literature [55] to clarify the problems and our goals. Let us consider a two-dimensional fermion system described by the Dirac Hamiltonian with a mass m. We put a U(1) gauge flux located at the origin, whose vector potential is given by

$$A_1(x,y) = -\alpha\frac{y}{r^2}, \quad A_2(x,y) = \alpha\frac{x}{r^2}, \tag{8}$$

where $r^2 = x^2 + y^2$ and the index i $(=1,2)$ of A_i denotes the direction of the vector (x and y components). The field strength describing the vortex or a point-like flux at the origin is

$$F_{12} = \partial_1 A_2 - \partial_2 A_1 = 2\pi\alpha\delta(x)\delta(y). \tag{9}$$

The Dirac Hamiltonian with the polar coordinate (r,θ) is

$$\begin{aligned} H &= \sigma_3\left(\sum_{i=1,2}\sigma_i(\partial_i - iA_i) + m\right) \\ &= \sigma_3\begin{pmatrix} m & e^{-i\theta}\left(\frac{\partial}{\partial r} - i\frac{1}{r}\frac{\partial}{\partial\theta} - \frac{\alpha}{r}\right) \\ e^{i\theta}\left(\frac{\partial}{\partial r} + i\frac{1}{r}\frac{\partial}{\partial\theta} + \frac{\alpha}{r}\right) & m \end{pmatrix}. \end{aligned} \tag{10}$$

Noting that H conserves the angular momentum $J = -i\frac{\partial}{\partial\theta} + \frac{1}{2}\sigma_3$, the general solution for $H\psi^{E,j} = E\psi^{E,j}$ at $r \neq 0$, which exponentially decays at large r is given by

$$\psi^{E,j}(r,\theta) = C\begin{pmatrix} (m+E)K_{j-\frac{1}{2}-\alpha}(\sqrt{m^2-E^2}r)e^{i(j-\frac{1}{2})\theta} \\ \sqrt{m^2-E^2}K_{j+\frac{1}{2}-\alpha}(\sqrt{m^2-E^2}r)e^{i(j+\frac{1}{2})\theta} \end{pmatrix}, \tag{11}$$

where C is the normalization constant and j is an eigenvalue of J, taking a half integer: $j \in \frac{1}{2} + \mathbb{Z}$.

In the $r = 0$ limit, the Bessel function is expanded as $K_\nu(Mr) \sim O(1/r^{|\nu|})$, and the solution $\psi^{E,j}(r,\theta)$ is normalizable only when $j = \alpha$.[4] The U(1) flux which allows the bound state of the electron is thus quantized.

[4]Note that $\int_{r_1} drrr^{-2\beta}$ is finite in the $r_1 \to 0$ limit only when $\beta \leqslant 1/2$.

The energy E must be also quantized since the wave function is limited in a tiny region around $r = 0$. If we smear the δ function in a region $r \sim r_1$, the energy will be discretized in units of $1/r_1$. From the condition $E^2 < m^2$, the only surviving energy value in the $r_1 \to 0$ limit is $E = 0$.

To summarize, for the vortex with $\alpha = 1/2 + n$ with $n \in \mathbb{Z}$, the system can have a unique square-integrable mode localized at the vortex,

$$\psi^{E=0,(2n+1)/2}(r,\theta) = C\begin{pmatrix} m \\ |m|e^{i\theta} \end{pmatrix}e^{in\theta}K_{\frac{1}{2}}(|m|r), \tag{12}$$

whose energy is zero. It is important to note that this mode is a "chiral" eigenstate of

$$\sigma_r = \frac{x}{r}\sigma_1 + \frac{y}{r}\sigma_2 = \begin{pmatrix} 0 & e^{-i\theta} \\ e^{i\theta} & 0 \end{pmatrix}, \tag{13}$$

with the eigenvalue $\mathrm{sign}(m)$.

The solution explains that the vortex can capture an electron state without any energy loss, with which we can interpret that the vortex is "charged." However, it is not sufficient to fully explain the physics in detail. First, the solution does not describe why this happens in the topological insulator with $m < 0$ but does not in the normal insulator ($m > 0$). One may impose a boundary condition $\sigma_r\psi = \mathrm{sign}(m)\psi$ by hand for the topological insulator and $\sigma_r\psi = -\mathrm{sign}(m)\psi$ for the normal insulator, but the choice looks ad hoc and any relation to the U(1) gauge flux is unclear. Second, the solution is square-integrable but its radial derivative $\partial_r\psi$ is not. This may be related to the singularity of the U(1) gauge field but it is difficult to identify the origin. Third, the Witten effect suggests that the charge that the defect gains is a half integer. But the above solution does not have any information about the fractional charge.

B. Wilson term and smearing of the U(1) flux

In the standard perturbative computation in continuum theory, we take the Dirac equation as it is in the classical field theory but higher derivative terms are introduced through the Pauli-Villars or heat-kernel regularization to make loop integrals finite. In lattice gauge theory, on the other hand, we must regularize the Dirac operator with the so-called Wilson term. The Wilson term corresponds to a covariant Laplacian, which is needed even at the tree level to avoid fermion doubling.

The Wilson term can be interpreted as a correction from the Pauli-Villars (PV) field in Eq. (1). The "regularized" Dirac operator is given by

$$D_{\mathrm{reg}} = M_{\mathrm{PV}}\frac{D+m}{D+M_{\mathrm{PV}}} = D + m - \frac{1}{M_{\mathrm{PV}}}D_\mu D^\mu, \tag{14}$$

where $O(1/M_{\mathrm{PV}}^2)$, $O(m/M_{\mathrm{PV}})$, and $O(F_{\mu\nu}/M_{PV})$ terms are omitted. Note that the overall factor M_{PV} is multiplied to keep the standard normalization. If we identify $1/M_{\mathrm{PV}}$ as the lattice spacing, the additional term corresponds to the Wilson term.

The Wilson term seems to play no role in the continuum limit $M_{\mathrm{PV}} \to \infty$ because it monotonically vanishes. However, as shown below, when the gauge field is focused in a smaller range compared with $1/M_{\mathrm{PV}}$, it gives a nontrivial effect. It is important to note that the sign of the mass m is well defined once the sign of M_{PV} is fixed. The Dirac equation is manifestly different between positive and negative m. As mentioned in

the previous sections, negative m represents the topological insulator, while $m > 0$ is in the trivial phase.

In the following analysis, we consider the Dirac Hamiltonian rather than the Dirac operator containing temporal derivative. The Wilson term is introduced only for the spatial directions, which corresponds to taking the continuum limit in the time direction first.[5]

Let us also regularize the gauge field by considering the U(1) flux with a finite size:

$$\begin{aligned} A_1(x,y) &= -\alpha\frac{y}{r_1^2}, \quad A_2(x,y) = \alpha\frac{x}{r_1^2} \text{ (for } r \leqslant r_1\text{)}, \\ A_1(x,y) &= -\alpha\frac{y}{r^2}, \quad A_2(x,y) = \alpha\frac{x}{r^2} \text{ (for } r > r_1\text{)}, \end{aligned} \tag{15}$$

where we assume $r_1 < 1/M_{\mathrm{PV}}$. The field strength F_{12} is zero outside of the circle $r > r_1$, while it is smeared to a constant $F_{12} = 2\alpha/r_1^2$ inside $r \leqslant r_1$, keeping the total flux

$$\int_{r<r_1} d^2x F_{12} = 2\pi\alpha \tag{16}$$

unchanged. In the polar coordinate, it is equivalent to setting the gauge field in the angular direction by

$$A_\theta = \begin{cases} \frac{\alpha r}{r_1^2} & (\text{for } r \leqslant r_1) \\ \frac{\alpha}{r} & (\text{for } r > r_1). \end{cases} \tag{17}$$

Note that the vector potential is regular at $r = 0$. In the above setup, the covariant Laplacian is given by

$$D_iD^i = \frac{\partial^2}{\partial r^2} + \frac{1}{r}\frac{\partial}{\partial r} - \left(-i\frac{1}{r}\partial_\theta - A_\theta\right)^2. \tag{18}$$

C. Solving the regularized Dirac equation

We are now ready to solve the regularized Dirac equation

$$H_{\mathrm{reg}}\psi = \left[H - \frac{1}{M_{\mathrm{PV}}}\sigma_3 D_iD^i\right]\psi = E\psi, \tag{19}$$

where we denote the energy by E. Since the system still respects the rotational symmetry: the modified Dirac Hamiltonian commutes with $J = -i\frac{\partial}{\partial\theta} + \frac{1}{2}\sigma_3$, so we can take the eigenfunction in the form

$$\psi^{E,j} = \begin{pmatrix} f(r)e^{i\theta(j-1/2)} \\ g(r)e^{i\theta(j+1/2)} \end{pmatrix}, \tag{20}$$

where j takes a half integer. On the (f, g) space, H_{reg} acts as

$$\begin{pmatrix} m - \frac{1}{M_{\mathrm{PV}}}\left[\frac{\partial^2}{\partial r^2} + \frac{1}{r}\frac{\partial}{\partial r} - \left(\frac{j-1/2}{r} - A_\theta\right)^2\right] & \frac{\partial}{\partial r} + \left(\frac{j+1/2}{r} - A_\theta\right) \\ -\frac{\partial}{\partial r} + \left(\frac{j-1/2}{r} - A_\theta\right) & -m + \frac{1}{M_{\mathrm{PV}}}\left[\frac{\partial^2}{\partial r^2} + \frac{1}{r}\frac{\partial}{\partial r} - \left(\frac{j+1/2}{r} - A_\theta\right)^2\right] \end{pmatrix}. \tag{21}$$

1. Solution at $r > r_1$

In the region $r > r_1$, $A_\theta = \alpha/r$. Noting that the modified Bessel equation guarantees that $K_\nu(\kappa r)$ [as well as $I_\nu(\kappa r)$] for any positive value of κ is the eigenstates of the Laplacian:

$$\left[\frac{\partial^2}{\partial r^2} + \frac{1}{r}\frac{\partial}{\partial r} - \frac{\nu^2}{r^2}\right]K_\nu(\kappa r) = \kappa^2 K_\nu(\kappa r), \tag{22}$$

the solution to the Dirac equation can still be in the form

$$\begin{pmatrix} aK_{j-1/2-\alpha}(\kappa r) \\ bK_{j+1/2-\alpha}(\kappa r) \end{pmatrix}, \tag{23}$$

with the coefficients a and b.

The general solution is thus a linear combination of the two solutions

$$\psi_{\mathrm{out}}^{E,j}(r,\theta) = C\begin{pmatrix} \left(m + E - \frac{\kappa_-^2}{M_{\mathrm{PV}}}\right)K_{j-\frac{1}{2}-\alpha}(\kappa_- r)e^{i(j-\frac{1}{2})\theta} \\ \kappa_- K_{j+\frac{1}{2}-\alpha}(\kappa_- r)e^{i(j+\frac{1}{2})\theta} \end{pmatrix} + D\begin{pmatrix} \left(m + E - \frac{\kappa_+^2}{M_{\mathrm{PV}}}\right)K_{j-\frac{1}{2}-\alpha}(\kappa_+ r)e^{i(j-\frac{1}{2})\theta} \\ \kappa_+ K_{j+\frac{1}{2}-\alpha}(\kappa_+ r)e^{i(j+\frac{1}{2})\theta} \end{pmatrix}, \tag{24}$$

with the coefficients C and D, where

$$\kappa_\pm = M_{\mathrm{PV}}\sqrt{\frac{(1 + 2m/M_{\mathrm{PV}}) \pm \sqrt{(1 + 2m/M_{\mathrm{PV}})^2 - 4(m^2 - E^2)/M_{\mathrm{PV}}^2}}{2}}. \tag{25}$$

The other two solutions given by I_ν are not square integrable at $r \to \infty$.

[5]In our study where $A_0 = 0$ and A_1 and A_2 are t independent, there is no contribution from the temporal covariant derivative.

2. Solution at $r \leqslant r_1$

Next, we consider the $r \leqslant r_1$ region. In this case, $A_\theta = \alpha r/r_1^2$ and the covariant Laplacian operates as

$$D_i D^i = \frac{\partial^2}{\partial r^2} + \frac{1}{r}\frac{\partial}{\partial r} - \frac{1}{r^2}\left[\left(j \mp \frac{1}{2}\right) - \frac{\alpha r^2}{r_1^2}\right]^2, \tag{26}$$

to the $\sigma_3 = \pm 1$ component.

Let us look at the upper spinor component $f(r)$. Assuming $j > 0$ and taking the form

$$f(r) = a r^{j-1/2} e^{-\frac{\alpha r^2}{2r_1^2}} F(r), \tag{27}$$

with a constant a, we find with the change of the variable $t = \alpha r^2/r_1^2$ that

$$D_i D^i f(r) = a r^{j-1/2} e^{-\frac{\alpha r^2}{2r_1^2}} \frac{4\alpha}{r_1^2}\left[t\frac{\partial^2}{\partial t^2} + \left\{\left(j+\frac{1}{2}\right) - t\right\}\frac{\partial}{\partial t} - \left(-\frac{r_1^2}{4\alpha}L\right)\right]F(r) + a r^{j-1/2} e^{-\frac{\alpha r^2}{2r_1^2}}\left(-L - \frac{2\alpha}{r_1^2}\right)F(r), \tag{28}$$

where we can take an arbitrary constant L (which cancels out at the right-hand side). If we take $F(r)$ to be a confluent hypergeometric function: $F_1(-r_1^2 L/4\alpha, j+1/2; \alpha r^2/r_1^2)$, then the first term vanishes and $f(r)$ is an eigenstate of the Laplacian:

$$D_i D^i f(r) = \left(-L - \frac{2\alpha}{r_1^2}\right) f(r). \tag{29}$$

Taking the lower spinor component as

$$g(r) = b\frac{L}{2j+1} r^{j+1/2} e^{-\frac{\alpha r^2}{2r_1^2}} {}_1F_1\left(-r_1^2 L/4\alpha + 1, j+3/2; \alpha r^2/r_1^2\right), \tag{30}$$

the Dirac equation is in a closed form[6] with respect to the coefficients (a, b):

$$\begin{pmatrix} m + \frac{1}{M_{\rm PV}}\left(L + \frac{2\alpha}{r_1^2}\right) & L \\ 1 & -m - \frac{1}{M_{\rm PV}}\left(L - \frac{2\alpha}{r_1^2}\right) \end{pmatrix}\begin{pmatrix} a \\ b \end{pmatrix} = E\begin{pmatrix} a \\ b \end{pmatrix}. \tag{35}$$

Note that the same equation is obtained for negative j. The general solution is thus a linear combination of the two solutions

$$\psi_{\rm in}^{E,j}(r,\theta) = A\begin{pmatrix} \left(m + E + \frac{L_-}{M_{\rm PV}} - \frac{2\alpha}{M_{\rm PV} r_1^2}\right) f_-^j(r) e^{i(j-\frac{1}{2})\theta} \\ g_-^j(r) e^{i(j+\frac{1}{2})\theta} \end{pmatrix} + B\begin{pmatrix} \left(m + E + \frac{L_+}{M_{\rm PV}} - \frac{2\alpha}{M_{\rm PV} r_1^2}\right) f_+^j(r) e^{i(j-\frac{1}{2})\theta} \\ g_+^j(r) e^{i(j+\frac{1}{2})\theta} \end{pmatrix}, \tag{36}$$

with constant coefficients A and B, where

$$L_\pm = M_{\rm PV}^2\left[\frac{-(1 + 2m/M_{\rm PV}) \pm \sqrt{(1+2m/M_{\rm PV})^2 - 4\left\{m^2 - \left(E - \frac{2\alpha}{M_{\rm PV} r_1^2}\right)^2\right\}/M_{\rm PV}^2}}{2}\right], \tag{37}$$

and

$$f_\pm^j(r) = \begin{cases} r^{j-1/2} e^{-\frac{\alpha r^2}{2r_1^2}} {}_1F_1\left(-r_1^2 L_\pm/4\alpha, j+1/2; \alpha r^2/r_1^2\right) & (\text{for } j > 0) \\ r^{-j+1/2} e^{-\frac{\alpha r^2}{2r_1^2}} {}_1F_1\left(-r_1^2 L_\pm/4\alpha - j + 1/2, -j+3/2; \alpha r^2/r_1^2\right) & (\text{for } j < 0), \end{cases} \tag{38}$$

$$g_\pm^j(r) = \begin{cases} \frac{L_\pm}{2j+1} r^{j+1/2} e^{-\frac{\alpha r^2}{2r_1^2}} {}_1F_1\left(-r_1^2 L_\pm/4\alpha + 1, j+3/2; \alpha r^2/r_1^2\right) & (\text{for } j > 0) \\ (2j-1) r^{-j-1/2} e^{-\frac{\alpha r^2}{2r_1^2}} {}_1F_1\left(-r_1^2 L_\pm/4\alpha - j + 1/2, -j+1/2; \alpha r^2/r_1^2\right) & (\text{for } j < 0). \end{cases} \tag{39}$$

---

[6] In the computations, we have used the following formulas about the confluent hypergeometric functions (here we omit the subscripts):

$$\partial_z F(\alpha, \gamma; z) = \frac{\alpha}{\gamma} F(\alpha+1, \gamma+1; z), \tag{31}$$

$$z\partial_z F(\alpha, \gamma+1; z) = \gamma[F(\alpha, \gamma; z) - F(\alpha, \gamma+1; z)], \tag{32}$$

$$zF(\alpha+1, \gamma+1; z) = (1 - \gamma/\alpha) F(\alpha, \gamma+1; z) + \frac{\gamma}{\alpha} F(\alpha, \gamma; z), \tag{33}$$

$$(\alpha - \gamma) F(\alpha, \gamma+1; z) = \alpha F(\alpha+1, \gamma+1; z) - \gamma F(\alpha, \gamma; z). \tag{34}$$

The other two solutions given by Tricomi's hypergeometric function $\mathrm{U}(a, b, z)$ are not square integrable.

3. Connecting in and out

Let us connect the exact solutions at $r = r_1$. In the standard analysis, one requires the eigenfunction and its first derivative to be continuous. In the above case where both solutions are eigenfunctions of the Laplacian, it is equivalent to impose the two conditions

$$\psi_{\mathrm{in}}^{E,j}(r_1,\theta) = \psi_{\mathrm{out}}^{E,j}(r_1,\theta), \quad D_iD^i\psi_{\mathrm{in}}^{E,j}(r_1,\theta) = D_iD^i\psi_{\mathrm{out}}^{E,j}(r_1,\theta), \tag{40}$$

together with the normalization condition to determine the coefficients A, B, C, D and the energy eigenvalue E.

In the limit $|M_{\mathrm{PV}}| \ll 1/r_1$, we can analytically show the existence of a deep bound state near $E \approx 0$. To this end, let us first rewrite the eigenfunction as

$$\psi_{\mathrm{in}}^{E,j}(r_1,\theta) = A\psi_{\mathrm{in}}^{-} + B\psi_{\mathrm{in}}^{+}, \quad \psi_{\mathrm{out}}^{E,j}(r_1,\theta) = C\psi_{\mathrm{out}}^{-} + D\psi_{\mathrm{out}}^{+}, \tag{41}$$

and that with the Laplacian multiplied accordingly. The explicit form for each component is given in Eqs. (24) and (36). In order for the coefficients A, B, C, D to have nontrivial solutions, the energy E must satisfy

$$\det\begin{pmatrix} \psi_{\mathrm{in}}^{-} & \psi_{\mathrm{in}}^{+} & -\psi_{\mathrm{out}}^{-} & -\psi_{\mathrm{out}}^{+} \\ D_iD^i\psi_{\mathrm{in}}^{-} & D_iD^i\psi_{\mathrm{in}}^{+} & -D_iD^i\psi_{\mathrm{out}}^{-} & -D_iD^i\psi_{\mathrm{out}}^{+} \end{pmatrix} = 0. \tag{42}$$

In the $|M_{\mathrm{PV}}| \ll 1/r_1$ limit[7] where $L_{\pm} \sim \pm 2\alpha/r_1^2 - M_{\mathrm{PV}}(M_{\mathrm{PV}} + 2m)/2$, a term containing the lower component of $D_iD^i\psi_{\mathrm{in}}^{-}$ and the upper component of $D_iD^i\psi_{\mathrm{in}}^{+}$ gives the dominant contribution to the determinant. Therefore, Eq. (42) reduces to

$$\det(-\psi_{\mathrm{out}}^{-} - \psi_{\mathrm{out}}^{+}) = 0, \tag{43}$$

which requires ψ_{out}^{-} and ψ_{out}^{+} to be parallel to each other.

It is important to note that, when $\alpha = j$, the Dirac operator becomes real: $\sigma_3 H^* = (\sigma_1 e^{-i(2j\theta)})^{-1}\sigma_3 H(\sigma_1 e^{-i(2j\theta)})$. For the one-dimensional edge modes, this real structure is identified as the T symmetry. Since $H^* = -(\sigma_1 e^{-i(2j\theta)})^{-1} H(\sigma_1 e^{-i(2j\theta)})$, any eigenmode of H with a nonzero eigenvalue λ: $H\psi_\lambda = \lambda\psi_\lambda$, makes a pair with $\sigma_1 e^{-i(2j\theta)}\psi_\lambda^*$, whose eigenvalue is $-\lambda$. Therefore, if the eigenvalue below $|m|$ is unique, $E = 0$ is the only possible choice, to keep the spectrum $\pm$ symmetric.

Let us explicitly confirm the above argument by taking the $r_1 \to 0$ limit and $\alpha - [\alpha] = (1+\epsilon)/2$, while keeping m and M_{PV} arbitrary under the condition $mM_{\mathrm{PV}} < 0$. The condition (43) leads to

$$\frac{\kappa_+^{1+\epsilon} - \kappa_-^{1+\epsilon}}{\kappa_+^{-1+\epsilon} - \kappa_-^{-1+\epsilon}} = M_{\mathrm{PV}}(m - E). \tag{44}$$

In the small-ϵ expansion, the energy is given by

$$E = \epsilon \frac{2|m|}{\sqrt{1 + 4m/M_{\mathrm{PV}}}} \ln\left[\frac{1 + \sqrt{1 + 4m/M_{\mathrm{PV}}}}{\sqrt{1 + 4m/M_{\mathrm{PV}}}}\right], \tag{45}$$

which becomes zero in the $\epsilon \to 0$ limit.

In the same $r_1 \to 0$ limit with finite M_{PV} and m, setting $\alpha = j$ (and $E = 0$), let us also compute the coefficients A, B, C, and D. It is sufficient to consider the angle $\theta = 0$. In this limit, we have $\kappa_\pm = M_{\mathrm{PV}}(1 \pm \sqrt{1 + 4m/M_{\mathrm{PV}}})/2$ (where we have assumed $m < 0$) and $(m - \kappa_\pm^2/M) = -\kappa_\pm$. From the connection condition for $D_iD^i\psi_{\mathrm{in}}^{E=0,j}(r_1, \theta = 0)$ and $D_iD^i\psi_{\mathrm{out}}^{E=0,j}(r_1, \theta = 0)$, we obtain

$$A = r_1^{3-j}A' \frac{(j + 1/2)e^{j/2}}{(2j)^2 {}_1F_1(3/2, j + 3/2; j)},$$
$$B = r_1^{2-j}A' \frac{e^{j/2}}{jM_{\mathrm{PV}} {}_1F_1(-1/2, j + 1/2; j)}, \tag{46}$$

with

$$A' = -\sqrt{\frac{\pi}{2}}\left(C\kappa_-^{5/2} + D\kappa_+^{5/2}\right). \tag{47}$$

It is interesting to note that we can immediately conclude $\psi_{\mathrm{in}}^{E=0,j}(r_1, \theta) = 0$ in the limit $r_1 = 0$ with the coefficients A and B above. Then we finally obtain from the condition $0 = \sqrt{r_1}\psi_{\mathrm{out}}^{E=0,j}(r_1, \theta = 0)$ that $D = -\sqrt{\kappa_-/\kappa_+}C$ and the bound state's eigenfunction is

$$\psi_{\mathrm{out}}^{E=0,j}(r, \theta) = C'[\sqrt{\kappa_-}K_{\frac{1}{2}}(\kappa_- r) - \sqrt{\kappa_+}K_{\frac{1}{2}}(\kappa_+ r)] \times \begin{pmatrix} e^{i(j-1/2)\theta} \\ -e^{i(j+1/2)\theta} \end{pmatrix}, \tag{48}$$

where $C' = -C\sqrt{\kappa_-}$ is a dimensionless normalization constant, which agrees with the solution obtained by Ref. [30].

Note in the large-M_{PV} limit, $\kappa_+ \to M_{\mathrm{PV}}$ while $\kappa_- \to |m|$. Therefore, the κ_+ component decays quickly and the only κ_- component survives converging to Eq. (11).

D. Microscopic understanding and why the charge is fractional

We have obtained an exact solution of the regularized Dirac equation with the Wilson term with a finite radius r_1 of the U(1) flux. Here we give a microscopic interpretation of the results.

The Wilson term makes the sign of the fermion mass well defined. Since every eigenvalue of the covariant Laplacian $-D_iD^i$ is positive for any configuration of the gauge field, inside topological insulators or in the case $m < 0$ taking M_{PV} positive, it is possible to locally flip the sign of the "effective" mass of the fermion

$$m_{\mathrm{eff}} = \left\langle m + \frac{-D_iD^i}{M_{\mathrm{PV}}} \right\rangle, \tag{49}$$

by a strong magnetic flux. In Ref. [48], we numerically confirmed that the vortex makes a small island of the positive-mass region.

With the U(1) flux analyzed above, the solution at $r < r_1$ has a dominant component whose eigenvalue of $-D_iD^i$ is $O(1/r_1)$. Therefore, for any value $m < 0$, the $r_1 \to 0$ limit guarantees creation of a domain wall around $r = r_1$ on which

[7] A simpler limit $m \ll |M_{\mathrm{PV}}| \ll 1/r_1$ was investigated in Ref. [48] by two of the authors.

a single chiral edge-localized mode appears, while the wall never appears inside normal insulators with $m > 0$. This is the unique bound state that the vortex captures in the topological insulators. The sharp change of the mass can be identified as the origin of the steep r dependence of the wave function.

Moreover, when $\alpha = \frac{1}{2} \bmod \mathbb{Z}$, the Dirac operator becomes real in the $r_1 \to 0$ limit. Then the binding energy must be zero to make the spectrum $\pm$ symmetric. For the one-dimensional edge-localized effective Hamiltonian, this is the T-symmetric point where the T transformation is given by the complex-conjugate operation. For this real Dirac operator, the number of zero modes is a topological invariant known as the mod-two Atiyah-Singer index [51].

To discuss the topological feature of the fermion zero mode, we also need an infrared regularization of the whole system. So far we have assumed an infinite flat space $\mathbb{R}^2$. In particle physics, the system is often regularized by the one-point compactification identifying the infinite points $r = \infty$. However, this does not work in our case. If we succeeded in the one-point compactification, the topological insulator $m_{\text{eff}} < 0$ region would have a topology of a disk with a small S^1 boundary at $r = r_1$. This contradicts the fact that the mod-two AS index is a cobordism invariant, which cannot be nonzero if the target manifold is a boundary of some higher-dimensional manifold. The resolution is given by setting the $m > 0$ region outside to create another domain wall at, say, $r = r_0$. In physics, this treatment is obvious since for any topological insulator, there exists its outside in the normal phase.[8]

Once the new domain wall is set, the cobordism requires another zero mode at $r = r_0$ to keep the total index trivial. Then the two zero eigenmodes, the bound state at the vortex and the one at the new domain-wall, mix by tunneling effect and the eigenvalues are split to some symmetric small values $\pm\varepsilon$ (still keeping the T symmetry of the edges). The edge-localized modes on a domain wall with radius $r_0 \gg r_1$ were analytically obtained in Ref. [48] by two of the authors. The zero-energy mode at $\alpha = j$ is a chiral eigenstate with $\sigma_r = +1$, which is opposite to that the solution in Eq. (48) has.

Fifty percent of the mixed state is located at the vortex, while the other 50% is sitting at the domain wall. In Ref. [48], two of the authors numerically confirmed this splitting on a square lattice. For the half filling situation where we put the Fermi energy to zero, only one of the two split zero modes is occupied. Then the charge expectation value around the vortex is $-1/2$ of the unit charge, while the other $-1/2$ is distributed on the surface of the topological insulator.

This is our microscopic interpretation of the mechanism how the vortex in the two-dimensional topological insulator gains a half of the electric charge. As shown below, the same mechanism explains the Witten effect whereby a magnetic monopole in a three-dimensional topological insulator becomes a dyon with a half-integral electric charge.

[8]Another consistent treatment is to put the same number of vortices and antivortices with an even number of domain walls in the system.

IV. A MONOPOLE IN THREE DIMENSIONS

Next let us consider a magnetic monopole in three dimensions. The vector potential of the Dirac monopole is given by

$$A_1 = \frac{-q_m y}{r(r+z)}, \quad A_2 = \frac{q_m x}{r(r+z)}, \quad A_3 = 0 \tag{50}$$

(the subscript 3 denotes the z direction), of which field strength is

$$\partial_i A_j - \partial_j A_i = q_m \epsilon_{ijk} \frac{x_k}{r^3} - 4\pi q_m \delta(x)\delta(y)\Theta(-z)\epsilon_{ij3}, \tag{51}$$

where we denote $(x_1, x_2, x_3) = (x, y, z)$. The second term represents the so-called Dirac string with the step function $\Theta(-z) = +1$ for $z \leqslant 0$, and $\Theta(-z) = 0$, otherwise. To eliminate the Dirac string, we may introduce another vector potential, which is regular in the thin cone around the Dirac string and glues to the first one, from which the quantization condition of the magnetic charge is required. However, in this work, we regard the Dirac string as a physical object between the monopole and antimonopole at a long distance. Here and in the following, we assume $q_m = n/2$ with an integer n.

When the Dirac string has no physical effect, the monopole configuration has an SO(3) rotational symmetry. Therefore, it is convenient to introduce the orbital angular momentum operator

$$L_i = -i\epsilon_{ijk} x_j (\partial_k - iA_k) - n\frac{x_i}{2r}, \tag{52}$$

which satisfies $[L_i, L_j] = i\epsilon_{ijk} L_k$. Their explicit form in the polar coordinate is given by

$$L_\pm = L_1 \pm iL_2 = e^{\pm i\phi}\left(\pm\frac{\partial}{\partial\theta} + i\frac{\cos\theta}{\sin\theta}\frac{\partial}{\partial\phi} + \frac{n}{2}\frac{\cos\theta - 1}{\sin\theta}\right), \tag{53}$$

$$L_3 = -i\frac{\partial}{\partial\phi} - \frac{n}{2}. \tag{54}$$

The highest and lowest states of L_3 are obtained from the equation $L_\pm g_\pm = 0$ as

$$g_+ = \sin^l\theta\left(\frac{1-\cos\theta}{1+\cos\theta}\right)^{\frac{n}{4}} e^{i(l+\frac{n}{2})\theta} = \left(\sin\theta e^{i\phi}\right)^{l+\frac{n}{2}} \times (1+\cos\theta)^{-\frac{n}{2}}, \tag{55}$$

$$g_- = \sin^l\theta\left(\frac{1+\cos\theta}{1-\cos\theta}\right)^{\frac{n}{4}} e^{i(l+\frac{n}{2})\theta} = \left(\sin\theta e^{-i\phi}\right)^{l-\frac{n}{2}} \times (1+\cos\theta)^{\frac{n}{2}}, \tag{56}$$

for which the two conditions $l \pm \frac{n}{2} \in \mathbb{Z}$ from the periodicity of ϕ, and $l - |\frac{n}{2}| \geqslant 0$ required from regularity at $\theta \to 0$, must be satisfied. Consequently, l must be a half integer not smaller than $|\frac{n}{2}|$, which is in contrast with the free-fermion case with an integer l.

A. Naive Dirac equation

With the monopole background obtained above, let us review the study of a bound state of the naive Dirac Hamiltonian

[36] without the Wilson term,

$$H = \gamma_0[\gamma^i(\partial_i - iA_i) + m] = \begin{pmatrix} m & \sigma^i(\partial_i - iA_i) \\ -\sigma^i(\partial_i - iA_i) & -m \end{pmatrix}, \tag{57}$$

where we have set $\gamma_0 = \sigma_3 \otimes 1$ and $\gamma_i = \sigma_1 \otimes \sigma_i$. It is important to note that H anticommutes with the "chirality"[9] operator $\bar{\gamma} = \sigma_1 \otimes 1$.

The orbital angular-momentum operator alone does not commute with the Dirac Hamiltonian but the total angular momentum

$$J_i = L_i + \tfrac{1}{2}\sigma_i, \quad [J_i, J_j] = i\epsilon_{ijk}J_k \tag{58}$$

does: $[1 \otimes J_i, H] = 0$ follows from $[J_i, \sigma^j(\partial_j - iA_j)] = 0$. Except for the lowest eigenvalue $j = |\frac{n}{2}| - 1/2$, where the degeneracy is $2j + 1 = |n|$, there are $2(2j + 1)$ degenerate states. In the following analysis, we use with $\sigma_r = x^j\sigma_j/r$ that

$$[J_i, \sigma_r] = 0, \quad \sigma^i L_i = J^2 - L^2 - 3/4. \tag{59}$$

There is another operator which commutes with H. To find this, let us define

$$D^{S^2} := \sigma^i\left(L_i + \frac{n}{2}\frac{x_i}{r}\right) + 1, \tag{60}$$

whose physical meaning will be discussed later. Using the equalities

$$[J_i, D^{S^2}] = 0, \quad \{D^{S^2}, \sigma_r\} = 0,$$
$$[D^{S^2}]^2 = \left(j + \frac{1}{2}\right)^2 - \frac{n^2}{4}, \tag{61}$$

it is not difficult to show $[\sigma_3 \otimes D^{S^2}, H] = 0$.

For $j > |\frac{n}{2}| - 1/2$ let us introduce the eigenstates of D^{S^2} which satisfies

$$D^{S^2}\chi_{j,j_3,\pm}(\theta,\phi) = \pm\sqrt{\left(j + \frac{1}{2}\right)^2 - \frac{n^2}{4}}\,\chi_{j,j_3,\pm}(\theta,\phi). \tag{62}$$

Then for any function $f(r)$ and $g(r)$, the vector of the form

$$\frac{1}{\sqrt{r}}\begin{pmatrix} f(r)\chi_{j,j_3,\pm}(\theta,\phi) \\ g(r)\sigma_r\chi_{j,j_3,\pm}(\theta,\phi) \end{pmatrix}, \tag{63}$$

is an eigenstate of $\sigma_3 \otimes D^{S^2}$. Here the overall factor $1/\sqrt{r}$ is introduced just for later convenience.

The $j = |\frac{n}{2}| - 1/2$ state we denote by $\chi_{j,j_3,0}$ is special and does not make a $\pm$ pair of D^{S^2}. We note that $\chi_{j,j_3,0}$ is an eigenstate of σ_r:

$$\sigma_r\chi_{j,j_3,0}(\theta,\phi) = \mathrm{sign}(n)\chi_{j,j_3,0}(\theta,\phi). \tag{64}$$

Since the degeneracy at each j is exhausted, the θ and ϕ dependence is completely obtained.

The remaining r dependence determines the energy eigenvalue E of H. For $j > |\frac{n}{2}| - 1/2$, we find no normalizable solution localized at the monopole. The only candidate for the bound state that the monopole can capture is, therefore, the state with $j = |\frac{n}{2}| - 1/2$, which should have the form

$$\frac{1}{r}\begin{pmatrix} f(r)\chi_{j,j_3,0}(\theta,\phi) \\ g(r)\chi_{j,j_3,0}(\theta,\phi) \end{pmatrix}, \tag{65}$$

and the equation reduces to

$$\begin{pmatrix} m & \mathrm{sign}(n)\partial_r \\ -\mathrm{sign}(n)\partial_r & -m \end{pmatrix}\begin{pmatrix} f(r) \\ g(r) \end{pmatrix} = E\begin{pmatrix} f(r) \\ g(r) \end{pmatrix}. \tag{66}$$

Noting that H^2 operates diagonally and identically on f and g, we can deduce that $g = \pm f$, or equivalently $\bar{\gamma} = \sigma_1 \otimes 1 = \pm 1$ and $E = 0$. The solution is $f(r) = \exp(-|m|r)$ and the possible bound state is, thus,

$$\frac{C_{j,j_3,0}}{r}\exp(-|m|r)\begin{pmatrix} 1 \\ \mathrm{sign}(m)\mathrm{sign}(n) \end{pmatrix}\chi_{j,j_3,0}(\theta,\phi), \tag{67}$$

which is a chiral eigenstate of $\sigma_1 \otimes \sigma_r$ with the eigenvalue $\mathrm{sign}(m)$. Here the normalization constant is denoted $C_{j,j_3,0}$.

For a unit magnetic charge $n = 1$, $j = j_3 = 0$ the possible bound state above is unique. However, we cannot distinguish normal and topological insulators unless we specify the chiral boundary condition at $r = 0$. In the above analysis, the origin of the chirality is not clear, either. In Ref. [36], a half electric charge is obtained by summing up all the charges in the Dirac sea and comparing with that without monopole, but only after a regularization which breaks conservation of the charge.

B. Wilson term

Let us introduce the Wilson term to the Dirac Hamiltonian in the presence of a monopole,

$$H = \gamma_0\left(\gamma^i(\partial_i - iA_i) + m - \frac{D_iD^i}{M_{\mathrm{PV}}}\right)$$
$$= \begin{pmatrix} m - D_iD^i/M_{\mathrm{PV}} & \sigma^i(\partial_i - iA_i) \\ -\sigma^i(\partial_i - iA_i) & -m + D_iD^i/M_{\mathrm{PV}} \end{pmatrix}. \tag{68}$$

First, we examine the symmetry of the modified Dirac Hamiltonian. Using

$$[\sigma^i(\partial_i - iA_i)]^2 = D_iD^i + \frac{n}{2r^2}\sigma_r, \tag{69}$$

$[J_i, \sigma_r] = 0$, and $[J_i, \sigma^j(\partial_j - iA_j)] = 0$ we can show that $[D_iD^i, J_i] = 0$ and the rotational symmetry is maintained: $[H, 1 \otimes J_i] = 0$.

However,

$$[D^{S^2}, D_iD^i] \neq 0, \tag{70}$$

which indicates that the $2(2j + 1)$ degenerate states for $j > |n/2| - 1/2$ are split into two $(2j + 1)$ degenerate sets.

It is remarkable that $\bar{\gamma} = \sigma_1 \otimes 1$ still anticommutes with H, which indicates that, if the bound state around the monopole is unique, its energy eigenvalue E must be zero and it must be a chiral eigenstate of $\bar{\gamma}$.

Before the exact calculation, let us determine the chirality of the bound state. Let us assume that $M_{\mathrm{PV}} > 0$, $m < 0$ and the point-like magnetic monopole charge is smeared in the region $r < r_1$. In a condensed-matter setup, the PV mass

[9] $\bar{\gamma}$ is different from the standard chirality operator $\gamma_5 = -\gamma_0\gamma_1\gamma_2\gamma_3 = \sigma_2 \otimes 1$. The extra symmetry with $\bar{\gamma}$ comes from absence of the scalar potential.

$M_{\rm PV}$ corresponds to the lattice spacing around 10^{-10} m between the atoms, while the size of the monopole is less than 10^{-20} m, assuming the monopole energy where the theory of 't Hooft–Polyakov [2,3] applies is higher than 10 TeV. From a dimensional analysis, $-D_iD^i \sim 1/r_1^2$ and under the condition $r_1 \ll 1/M_{\rm PV}$, it is natural to assume that $m_{\rm eff}(r) = \langle m - D_iD^i/M_{\rm PV}\rangle$ is effectively positive for some region near the origin, while it is kept negative at large r. Namely, a domain wall is created around the monopole. Then the bound state should satisfy[10]

$$[\sigma_1 \otimes \sigma_r \partial_r + m_{\rm eff}(r)]\psi = 0, \tag{71}$$

to which the normalizable solution is given by

$$\psi \sim \exp\left[\int_{r_1}^{r} dr' m_{\rm eff}(r')\right], \tag{72}$$

which requires $\sigma_1 \otimes \sigma_r = -1$. It is interesting to note that the both chiralities $\bar\gamma = \pm 1$ are possible as long as the lower-dimensional chirality takes the same eigenvalue $-1 \otimes \sigma_r = \pm 1$. This reflects the fact that the Atiyah-Singer index on the two-dimensional domain wall is not $\mathbb{Z}_2$ but $\mathbb{Z}$. In fact, we will show below that the index is equal to the magnetic charge n.

C. The solution to the regularized Dirac equation

Let us derive the bound state described by the regularized Dirac equation. Here we assume that $j = |n/2| - 1/2$, the edge-localized states have a chirality $\sigma_1 \otimes \sigma_r = -1$ at r_1, and take the $r_1 \to 0$ limit.

We employ the ansatz for the (nearest) zero modes to have the following form with $s = \mathrm{sign}(n)$:

$$\psi = \frac{f(r)}{r}\begin{pmatrix} 1 \\ -s \end{pmatrix} \otimes \chi_{j,j_3,0}(\theta,\phi), \tag{73}$$

which has a $2j+1 = |n|$ degeneracy, having different values of j_3. It is important to note that ψ is a simultaneous eigenstate of $-\bar\gamma = -\sigma_1 \otimes 1$ and $1 \otimes \sigma_r$ sharing the same eigenvalue s. From the anticommutation relation $\{H, \bar\gamma\} = 0$, one can conclude that the eigenvalue of H is exactly zero, as long as it is isolated.

With a further change of the functional form to $f(r) = \sqrt{r}e^{-M_{\rm PV}r/2}g(\kappa r)$ with $\kappa = M_{\rm PV}\sqrt{1+4m/M_{\rm PV}}/2$ it is not difficult to show that $g(\kappa r)$ satisfies the modified Bessel equation. Here we have assumed that $4|m|/M_{\rm PV} < 1$. Therefore, we obtain the general solution as

$$\psi = \frac{e^{-\frac{M_{\rm PV}r}{2}}}{\sqrt{r}}[AK_\nu(\kappa r) + BI_\nu(\kappa r)]\begin{pmatrix} 1 \\ -s \end{pmatrix} \otimes \chi_{j,j_3,0}(\theta,\phi), \tag{74}$$

where $\nu = (\sqrt{2|n|+1})/2$, with the constant coefficients A and B.

To connect ψ and $D_iD^i\psi \sim \psi/r$ (indicated by the Bessel equation) at finite $r = r_1$ and take the $r_1 \to 0$ limit, the steep $1/r_1$ dependence requires (in the same way as explicitly shown in the two-dimensional vortex case in Sec. III) that $A = O(r_1^\nu)$ (ψ vanishes at $r_1 \to 0$).

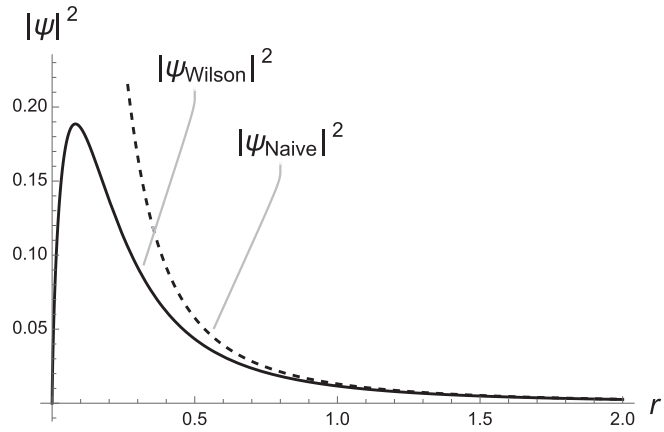

FIG. 1. The comparison of the solution with the Wilson term in Eq. (75) (solid curve) and the one in the previous work (dashed curve) in Eq. (67). Here we choose the parameters $n = 1$, $m = 0.1$, and $M_{\rm PV} = 10$.

We finally obtain the localized state to the monopole,[11]

$$\psi^{\rm mono}_{j,j_3} = \frac{Be^{-\frac{M_{\rm PV}r}{2}}}{\sqrt{r}}I_\nu(\kappa r)\begin{pmatrix} 1 \\ -s \end{pmatrix} \otimes \chi_{j,j_3,0}(\theta,\phi), \tag{75}$$

with a normalization constant B. As is expected, in the $M_{\rm PV} \to \infty$ limit, where $I_\nu(\kappa r) \sim \exp(\frac{M_{\rm PV}}{2}r - |m|r)/\sqrt{\pi r M_{\rm PV}}$, ψ converges to the naive Dirac solution in Eq. (67). The comparison of the two results is shown in Fig. 1 where we choose $n = 1$, $m = 0.1$, and $M_{\rm PV} = 10$. Remarkable differences is that the Wilson term yields a peak at $r = c_\nu/M_{\rm PV}$ with $c_\nu = (4\nu^2 - 1)/4 = |n|/2$ and makes the wave function zero at $r = 0$.

In contrast to the vortex system in Sec. III the magnetic field is nonzero even outside r_1. In fact, as shown in Fig. 1 the peak of the edge mode wave function in Eq. (75) is located at $r \sim 1/M_{\rm PV}$. The scale $1/M_{\rm PV}$ corresponds to the atomic lattice spacing $\approx 10^{-10}$ m of the topological insulator, which will be much larger than the size of the monopole $\approx 10^{-20}$ m. We conclude by this exact solution that the domain wall with a finite radius $r \sim 1/M_{\rm PV}$ is created by the monopole, on which the $|n|$ chiral edge modes appear with energy zero. These are the origin of the electric charge the magnetic monopole gains.

D. Atiyah-Singer index theorem and zero-mode pairing

In the previous section we obtained $|n| = 2j+1$ zero modes with the chirality $1 \otimes \sigma_r = s = \mathrm{sign}(n)$. The fact that these zero modes are located not on the point-singularity of the monopole but on a finite two-dimensional spherical domain wall makes the topological property of the solutions clearer. Note that they are also the zero modes of the operator $D^{S^2} = \sigma^i(L_i + \frac{n}{2}\frac{x_i}{r}) + 1$. In fact, this operator can be identified as the effective Dirac operator on the two-dimensional sphere

[10] Here we treat the effect of the Wilson term as a mean field for the Dirac equation. See the exact treatment in the next section.

[11] Our solution coincides the result obtained in Refs. [39,40] where the Wilson term is introduced but smearing of the point-like singularity of the monopole and dynamical mass shift were not considered.

around the monopole with a radius we denote by $r_2 \sim 1/M_{\rm PV}$. With a local Lorentz (or *Spin*^{c} to be precise) transformation $R(\theta,\phi) = \exp(i\theta\sigma_2/2)\exp[i\phi(\sigma_3+1)/2]$, we obtain

$$\frac{1}{r_2}D^{S^2} := \frac{1}{r_2}R(\theta,\phi)D^{S^2}R(\theta,\phi)^{-1} = -\frac{1}{r_2}\sigma_3\left[\sigma_1\frac{\partial}{\partial\theta} + \sigma_2\left(\frac{1}{\sin\theta}\frac{\partial}{\partial\phi} + i\hat{A}_\phi + i\hat{A}^s_\phi\right)\right], \tag{76}$$

where $\hat{A}_\phi = (n/2)[\sin\theta/(1+\cos\theta)]$ is the vector potential (in units of r_2) generated by the monopole, and

$$\hat{A}^s_\phi = \frac{1}{2\sin\theta} - \frac{\cos\theta}{2\sin\theta}\sigma_3, \tag{77}$$

is the induced *Spin*^{c} connection on the sphere, which is strongly curved with the small radius r_2 [48]. It is also important to note that the same transformation changes the chirality operator to $R(\theta,\phi)\sigma_r R(\theta,\phi)^{-1} = \sigma_3$. Namely, these zero modes are the chiral zero modes of D^{S^2}.

As shown in Ref. [48], the gravitational effect on a sphere generally gives a gap in the massless Dirac operator spectrum with a size of its inverse radius. The U(1) gauge connection from the monopole cancels the gravity to have the zero eigenvalues. Since the degeneracy of the zero modes is $|n|$ with the chirality $\sigma_3 = \mathrm{sign}(n)$, we can conclude that the index of the Dirac operator D^{S^2} is n.

Stability of the chiral zero modes is topologically protected by the AS index theorem. On the two-dimensional sphere of radius r_2, we can explicitly compute that

$$\frac{1}{4\pi}\int_{S^2} d^2x\epsilon^{\mu\nu}F_{\mu\nu} = n. \tag{78}$$

Note that the *Spin*^{c} connection $\hat{A}^s_\phi$ does not contribute to the index in two dimensions.

Since the AS index is a cobordism invariant, a similar discussion about the zero-mode pairing as in the case of the vortex in two dimensions in Sec. III applies here. The conventional one-point compactification of $r=\infty$ points does not work, since the magnetic flux coming from the monopole becomes infinitely dense again at the compactified point, which is equivalent to put another monopole with the opposite magnetic charge $q_m = -n/2$. This second monopole creates another domain wall, which is cobordant to the one around the original monopole. The argument implies that there must exist a region of normal phase before reaching $r=\infty$: outside of the topological insulator is always a normal insulator. On the outer domain wall, $|n|$ zero modes with the same chirality of $1\otimes\sigma_r$ as the monopole-localized zero modes must appear as a consequence of the cobordism invariance of the AS index.[12]

Let us consider another domain wall at large radius r_0, giving a position-dependent mass term $m(r) = |m|\epsilon(r-r_0)$ where $\epsilon(r-r_0) = \pm 1$ for $r \gtrless r_0$. The region $r > r_0$ corresponds to a normal insulator. The edge-localized state in each region is obtained as

$$\psi^{\rm DW}_{j,j_3} = \begin{cases} \frac{\exp\left(\frac{M_{\rm PV}r}{2}\right)}{\sqrt{r}}\left(e^{\kappa_- r_0}B'K_\nu(\kappa_- r) + e^{-\kappa_- r_0}C'I_\nu(\kappa_- r)\right)\begin{pmatrix}1\\ s\end{pmatrix}\otimes\chi_{j,j_3,0}(\theta,\phi), & (r<r_0) \\ \frac{D'\exp\left(\kappa_+ r_0 + \frac{M_{\rm PV}r}{2}\right)}{\sqrt{r}}K_\nu(\kappa_+ r)\begin{pmatrix}1\\ s\end{pmatrix}\otimes\chi_{j,j_3,0}(\theta,\phi), & (r>r_0), \end{cases} \tag{79}$$

where $\kappa_\pm = M_{\rm PV}\sqrt{1\pm 4|m|/M_{\rm PV}}/2$. The ratios C'/B' and D'/B' are determined from the connecting condition of the wave function, as well as that for its derivative at the domain wall $r=r_0$. In the large-$r_0 m$ limit, we find

$$\frac{C'}{B'} = \frac{\kappa_-[K_{\nu-1}(\kappa_- r_0) + K_{\nu+1}(\kappa_- r_0)]K_\nu(\kappa_+ r_0) - \kappa_+[K_{\nu-1}(\kappa_+ r_0) + K_{\nu+1}(\kappa_+ r_0)]K_\nu(\kappa_- r_0)}{\kappa_-[I_{\nu-1}(\kappa_- r_0) + I_{\nu+1}(\kappa_- r_0)]K_\nu(\kappa_+ r_0) + \kappa_+[K_{\nu-1}(\kappa_+ r_0) + K_{\nu+1}(\kappa_+ r_0)]I_\nu(\kappa_- r_0)}e^{2\kappa_- r_0} \sim \pi\frac{\kappa_- - \kappa_+}{\kappa_- + \kappa_+}, \tag{80}$$

and

$$\frac{D'}{B'} = \frac{\kappa_-\{[I_{\nu-1}(\kappa_- r_0) + I_{\nu+1}(\kappa_- r_0)]K_\nu(\kappa_- r_0) + [K_{\nu-1}(\kappa_- r_0) + K_{\nu+1}(\kappa_- r_0)]I_\nu(\kappa_- r_0)\}}{\kappa_-[I_{\nu-1}(\kappa_- r_0) + I_{\nu+1}(\kappa_- r_0)]K_\nu(\kappa_+ r_0) + \kappa_+[K_{\nu-1}(\kappa_+ r_0) + K_{\nu+1}(\kappa_+ r_0)]I_\nu(\kappa_- r_0)}e^{(\kappa_- - \kappa_+)r_0} \sim \frac{2\sqrt{\kappa_-\kappa_+}}{\kappa_- + \kappa_+}. \tag{81}$$

These edge-localized modes have the same $|n| = 2j+1$ degeneracy with the zero modes captured by the monopole but with the opposite chirality: $\sigma_1\otimes\sigma_r = +1$.

In the $M_{\rm PV} \gg m$ limit, the zero mode above takes a simpler form with $D'/B' \sim 1$ and $C'/B' \sim 0$:

$$\psi^{\rm DW}_{j,j_3} = \frac{B''}{r}\exp\left[-|m||r-r_0|\right]\begin{pmatrix}1\\ s\end{pmatrix}\otimes\chi_{j,j_3,0}(\theta,\phi). \tag{82}$$

[12]The cobordism invariance of the AS index can be understood by the Stokes theorem. Suppose ∂X_1 and $-\partial X_2$ (where the negative sign indicates the opposite orientation to X_1) are two disjoint boundaries of a three-dimensional manifold X. In the differential form, we can show $0 = \int_X dF = \int_{\partial X_1} F - \int_{-\partial X_2} F$.

At finite r_0, the paired zero mode (having the same j_z) near the monopole at r_1 and the domain wall r_0 mix to give symmetric splitting to the Dirac spectrum. Let us perturbatively estimate this mixing following the method given in Ref. [39]. When $|m|r_0$ is large enough, the zero mode around the monopole $\psi^{\text{mono}}_{j,j_3}$ in Eq. (75) and that near the domain wall ψ^{DW}_{j,j_3} in Eq. (79) are still approximate eigenstates of H. As the total angular momentum J_i commutes with H, each eigenstate of H after mixing the two is given by

$$\psi = \alpha\psi^{\text{mono}}_{j,j_3} + \beta\psi^{\text{DW}}_{j,j_3}, \tag{83}$$

where α and β are constants. Note here that $\psi^{\text{mono}}_{j,j_3}$ and ψ^{DW}_{j,j_3} are both eigenstates of the chirality operator $\bar{\gamma} = \sigma_1 \otimes 1$, which anticommutes with H. We can immediately obtain the diagonal parts $(\psi^{\text{mono}}_{j,j_3})^\dagger H \psi^{\text{mono}}_{j,j_3} = (\psi^{\text{DW}}_{j,j_3})^\dagger H \psi^{\text{DW}}_{j,j_3} = 0$. We can also show that the off-diagonal part is real and symmetric: $(\psi^{\text{mono}}_{j,j_3})^\dagger H \psi^{\text{DW}}_{j,j_3} = (\psi^{\text{DW}}_{j,j_3})^\dagger H \psi^{\text{mono}}_{j,j_3} =: \Delta$. Then we can show that $\alpha = \pm\beta$ and the split energy is $E = \pm\Delta$. This result, having 50% amplitude around the monopole, is valid at any large value of r_0. The normal insulator outside and the edge modes on it cannot be ignored from the theory no matter how long they are separated.

When we set the Fermi energy zero, only one of each zero-mode pairs is occupied. Since only a half of the amplitude is distributed around the monopole, the charge expectation value around $r = r_1$ will be $-|n|/2$, while the other half is spread on the surface at $r = r_0$. Thus we complete the microscopic description how the monopole gains a half electric charge. In the next section, we nonperturbatively examine the above scenario on a lattice taking r_0 finite.

V. NUMERICAL ANALYSIS OF MONOPOLE ON A LATTICE

In this section, we numerically investigate the monopole system in a topological insulator with a lattice regularization. In particular, we try to confirm creation of the domain wall, or the surface of a normal insulator island around the monopole. We will also quantify the zero-mode pairing of the monopole-captured state and the edge-localized state at the spherical domain wall with finite radius $r = r_0$ and their tunneling effects, as well as the electric charge expectation value around the monopole.

A. Lattice setup

On three-dimensional hyper-cubic lattices with size $L = 23$, 31, and 47 (where the number of sites in each direction is 24, 32, and 48, respectively), with open boundary conditions, we put a monopole at $\boldsymbol{x}_m = (x_m, y_m, z_m) = (L/2, L/2, L/2)$ with a magnetic charge $n/2$. We also put an antimonopole at $\boldsymbol{x}_a = (x_a, y_a, z_a) = (L/2, L/2, 1/2)$ with the opposite charge $-n/2$ to ensure the Gauss law constraint in the continuum limit. The continuum vector potential at $\boldsymbol{x} = (x, y, z)$ is then given by

$$\begin{aligned}
A_1(\boldsymbol{x}) &= q_m\left[\frac{-(y-y_m)}{|\boldsymbol{x}-\boldsymbol{x}_m|(|\boldsymbol{x}-\boldsymbol{x}_m|+(z-z_m))} - \frac{-(y-y_a)}{|\boldsymbol{x}-\boldsymbol{x}_a|(|\boldsymbol{x}-\boldsymbol{x}_a|+(z-z_a))}\right],\\
A_2(\boldsymbol{x}) &= q_m\left[\frac{(x-x_m)}{|\boldsymbol{x}-\boldsymbol{x}_m|(|\boldsymbol{x}-\boldsymbol{x}_m|+(z-z_m))} - \frac{(x-x_a)}{|\boldsymbol{x}-\boldsymbol{x}_a|(|\boldsymbol{x}-\boldsymbol{x}_a|+(z-z_a))}\right],\\
A_3(\boldsymbol{x}) &= 0,
\end{aligned} \tag{84}$$

with $q_m = n/2$. Note that the Dirac string extends from $\boldsymbol{x}_a$ to $\boldsymbol{x}_m$.

The link variables on the lattice is given by exponentiated line integrals of the vector potential:

$$U_j(\boldsymbol{x}) = \exp\left[i\int_0^1 A_j(\boldsymbol{x}')dl\right], \tag{85}$$

where $\boldsymbol{x} = (x, y, z)$ having integer-valued components denotes the lattice coordinate, and the line integral with respect to $\boldsymbol{x}' = \boldsymbol{x} + \boldsymbol{e}_j l$ where $\boldsymbol{e}_j$ is the unit vector in the j direction is taken from $\boldsymbol{x}$ to $\boldsymbol{x} + \boldsymbol{e}_j$ along the link. Here and in the following, we take the lattice spacing to be unity.

For the fermion field, we assign a position-dependent mass term $m(\boldsymbol{x}) = -m_0$ for $r = \sqrt{|\boldsymbol{x}-\boldsymbol{x}_m|} \leqslant r_0 = \frac{3}{8}L$ and $m(\boldsymbol{x}) = +m_0$ otherwise. The constant $m_0(L+1) = 14$ is fixed to take the continuum limit. In this setup, the monopole is located at the center of a spherical topological insulator with radius r_0, while the antimonopole sits in the normal insulator region with the mass $+m_0$. Outside of the lattice with open boundary condition corresponds to a "laboratory" with $m(\boldsymbol{x}) = +\infty$. Since the $m(\boldsymbol{x}) = +m_0$ region and that with $m(\boldsymbol{x}) = +\infty$ are both in the trivial phase, we do not expect any edge-localized modes to appear at the boundaries $x_{i=1,2,3} = 0$ or $x_{i=1,2,3} = L$. Our lattice setup with $L = 23$ is sketched in Fig. 2. The symbols "N" and "S" represent monopole and antimonopole, respectively, which are connected by the Dirac string shown by the thick line. Inside the spherical domain wall of radius $r_0 = 9$, we put a negative mass $-m_0 = -7/12$, while it is $+7/12$ outside.

The Wilson Dirac Hamiltonian is given by

$$H_W = \gamma^0\left(\sum_{i=1}^{3}\left[\gamma^i\frac{\nabla_i^f + \nabla_i^b}{2} - \frac{1}{2}\nabla_i^f\nabla_i^b\right] + m(\boldsymbol{x})\right), \tag{86}$$

where $\nabla_i^f\psi(\boldsymbol{x}) = U_i(\boldsymbol{x})\psi(\boldsymbol{x}+\boldsymbol{e}_i) - \psi(\boldsymbol{x})$ denotes the forward covariant difference and $\nabla_i^b\psi(\boldsymbol{x}) = \psi(\boldsymbol{x}) - U_i^\dagger(\boldsymbol{x}-\boldsymbol{e}_i)\psi(\boldsymbol{x}-\boldsymbol{e}_i)$ is the backward difference. The gamma matrices are the same as in the continuum: $\gamma_0 = \sigma_3 \otimes 1$, $\gamma_i = \sigma_1 \otimes \sigma_i$. It is important to note that H_W anticommutes with $\bar{\gamma} = \sigma_1 \otimes 1$ even on a lattice. In the analysis below, we compute the eigenvalues denoted by E_k and their eigenfunction $\phi_k(\boldsymbol{x})$ of

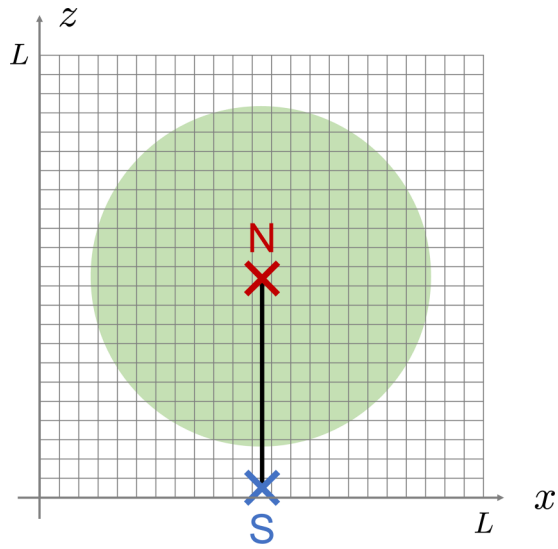

FIG. 2. Our lattice setup on a $L = 23$ lattice (at the $y = 0$ slice) is presented. The symbols "N" and "S" represent monopole and antimonopole, respectively, which are connected by the Dirac string shown by the thick line. Inside the shadowed sphere of radius $r_0 = 9$, we put a negative mass $-m_0 = -7/12$, while it is $+7/12$ outside.

H_W and study their local amplitude normalized by r^2,

$$A_k(\boldsymbol{x}) = \phi_k(\boldsymbol{x})^\dagger \phi_k(\boldsymbol{x}) r^2, \tag{87}$$

as well as the local distribution of operators.

B. Numerical results

In Fig. 3, we plot the Dirac eigenvalue spectrum on the $L = 31$ lattice in units of r_0 with circle symbols. On the left panel, the result with $n = 1$ is presented while that with $n = -2$ is shown in the right panel. Our results are consistent with a similar numerical analysis presented in Ref. [40]. For comparison, we also plot the continuum results (without the Wilson term) with crosses for the edge-localized modes on the domain wall at r_0. The gradation of the symbols for each eigenmode $\phi_k(\boldsymbol{x})$ represents the chirality expectation value measured by

$$\sum_{\boldsymbol{x}} \phi_k^\dagger(\boldsymbol{x})[\sigma_1 \otimes \sigma_r]\phi_k(\boldsymbol{x}). \tag{88}$$

The edge-localized modes between $\pm m_0$ have chirality $\sigma_1 \otimes \sigma_r \sim +1$, except for the modes in the vicinity of zero.

Let us focus on the (near) zero modes which are apparently not chiral. The number of these modes is doubled compared with the continuum prediction of the edge-localized modes around the domain wall $r = r_0$. As explained in the previous section, any chiral zero mode localized at the domain wall must appear in a pair with the mode with the opposite chirality localized at the inner domain wall dynamically created by the monopole. The paired chiral zero modes are mixed due to the tunneling effect. The near zero-mode doubling in our numerical data is consistent with this scenario. For the negative nearest-zero mode in the case of $n = 1$ [whose eigenfunction is denoted by $\phi_1(\boldsymbol{x})$] we plot in the left panel of Fig. 4 the amplitude $A_1(\boldsymbol{x})$ at the $z = (L + 1)/2$ slice. For comparison we also present the same plot in the right panel but for the second nearest-zero mode $A_2(\boldsymbol{x})$. The gradation of the symbols shows the local chirality,

$$\phi_k^\dagger(\boldsymbol{x})[\sigma_1 \otimes \sigma_r]\phi_k(\boldsymbol{x})/\phi_k^\dagger(\boldsymbol{x})\phi_k(\boldsymbol{x}), \tag{89}$$

with $k = 1$ or 2. We can see only in the left panel that the amplitude has two peaks around $r = |\boldsymbol{x} - \boldsymbol{x}_m| = 0$ and $r = r_0$ and the local chirality near each peak is ≈ -1 and $+1$, respectively, although the total chirality is close to zero.

Figure 5 shows the same amplitudes $A_0(\boldsymbol{x})$ (left panel) and $A_2(\boldsymbol{x})$ (right panel) but with $n = -2$ and at the $x = (L + 1)/2$ slice. As expected, these are the two near-zero modes whose wave function is partly captured by the monopole. However, the shape of the wave function becomes asymmetric due to the antimonopole located at $\boldsymbol{x}_a = (x_a, y_a, z_a) = (L/2, L/2, 1/2)$.

Next let us directly confirm creation of the domain wall near the monopole. Figure 6 plots the distribution of the "effective mass"(normalized by m_0) locally measured at the

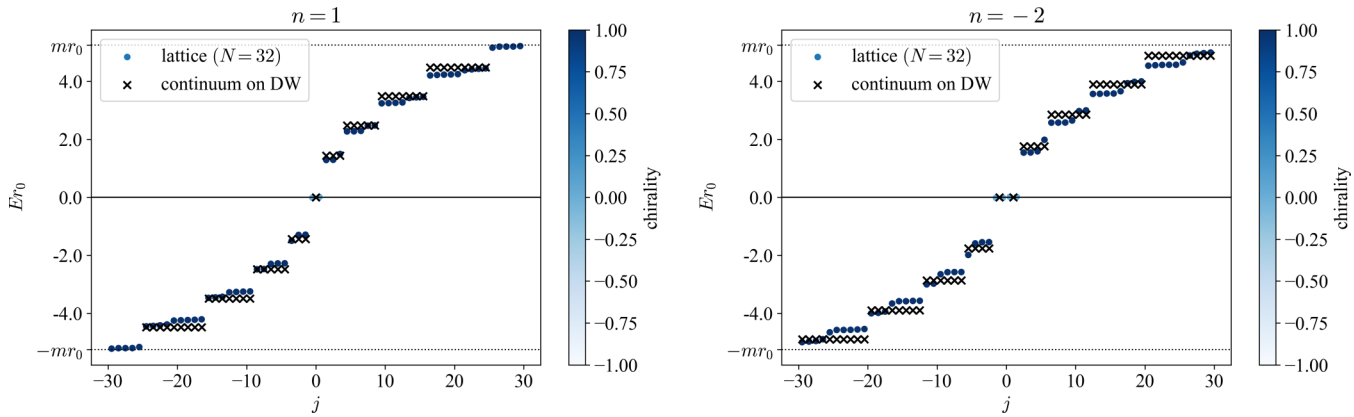

FIG. 3. Low-lying eigenvalue spectrum of H_W with the monopole charge $n = 1$ (left panel) and $n = -2$ (right panel). Circle symbols represent our lattice data, while crosses are continuum predictions for the edge-localized modes on the outer domain wall. See the main text for details of other numerical setups.

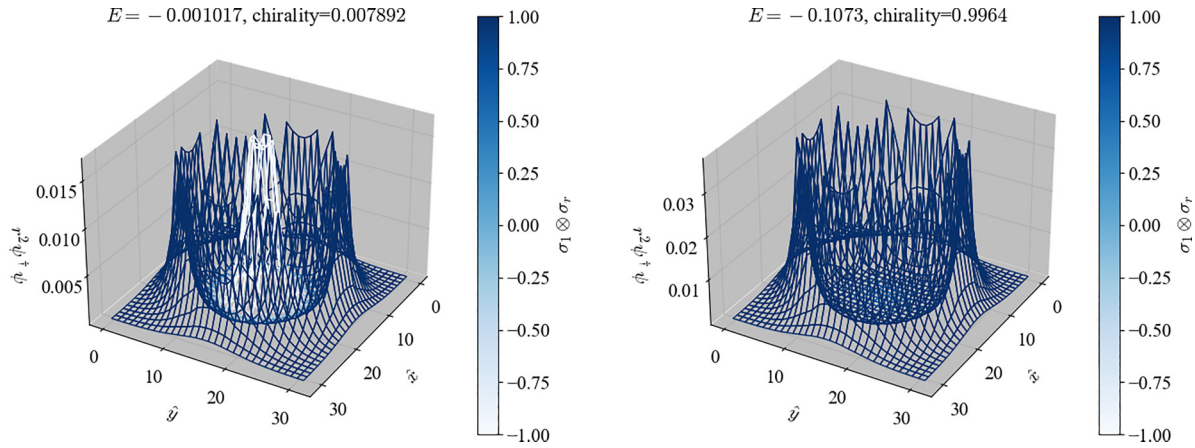

FIG. 4. (left panel) The amplitude of the negative nearest-zero mode $A_1(\boldsymbol{x})$ at the $z = (L+1)/2$ slice in the presence of a unit monopole $n = 1$ is plotted. (right panel) The same as the left panel but for the second negative nearest-zero mode $A_2(\boldsymbol{x})$. The gradation represents the locally measured chirality of $\sigma_1 \otimes \sigma_r$.

$z = (L+1)/2$ slice,

$$m_{\text{eff}}(\boldsymbol{x}) = \phi_1(\boldsymbol{x})^\dagger \left[-\sum_{i=1,2,3} \frac{1}{2} \nabla_i^f \nabla_i^b + m(\boldsymbol{x}) \right] \times \phi_1(\boldsymbol{x}) \Big/ \phi_1(\boldsymbol{x})^\dagger \phi_1(\boldsymbol{x}), \tag{90}$$

with a unit monopole charge $n = 1$ (left panel) and that with $n = -2$ (right panel). The data are shown with gradation to make explicit the two regions of normal phase with $m_{\text{eff}}/m_0 \sim +1$ in dark mesh and the one for topological phase with $m_{\text{eff}}/m_0 \sim -1$ in light mesh. We can see that a small island of a normal insulator or a positive mass region appears around the monopole, and we thus confirm that a domain wall is dynamically created.

As discussed above about Figs. 4 and 5, the distribution of the chirality $\sigma_1 \otimes \sigma_r$ has no significant difference between $n = 1$ and $n = -2$, i.e., the wave function near the monopole is $\sigma_1 \otimes \sigma_r \approx -1$, while that near the domain wall at $r = r_0$ has $\approx +1$ chirality. However, for the two-dimensional chiral operator $1 \otimes \sigma_r$, the result is sensitive to the sign of n. As shown in Fig. 7 where the distribution of

$$\phi_1^\dagger(\boldsymbol{x})[1 \otimes \sigma_r]\phi_1(\boldsymbol{x}) / \phi_1^\dagger(\boldsymbol{x})\phi_1(\boldsymbol{x}) \tag{91}$$

is indicated by the gradation of the plot, the local two-dimensional chirality is uniformly $\approx +1$ for $n = 1$ and ≈ -1 for $n = -2$. This is consistent with the cobordism property of the AS index that the spherical domain wall at $r = r_0$ and that near the monopole must share the same value n.

So far we have used the lattice size $L = 31$. To estimate the systematics due to the lattice spacing a, we also compute the Dirac eigenvalues on $L = 23$ and $L = 47$ lattices with the same physical setup. In Fig. 8 we present the lattice cut-off a/L dependence of negative nearest-zero eigenvalues. They show a mild linear dependence, which is comparable to what observed in the previous analysis in the free fermion case by two of the authors [47].

Finally let us quantify the electric charge that the monopole gains. In Fig. 9, we plot the cumulative distribution

$$C_k(r) = \int_{|\boldsymbol{x}|<r} d^3x \phi_k(\boldsymbol{x})^\dagger \phi_k(\boldsymbol{x}), \tag{92}$$

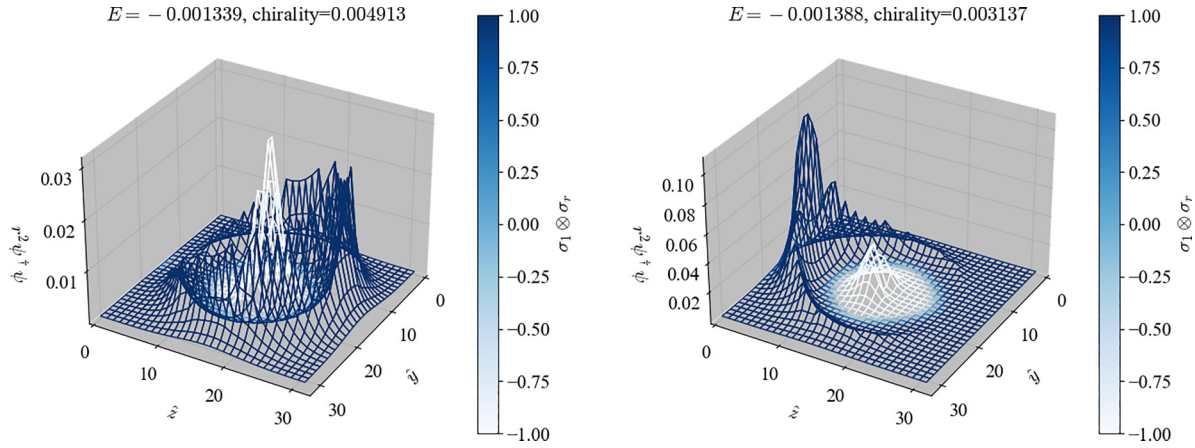

FIG. 5. (left panel) The amplitude of the negative nearest-zero mode $A_1(\boldsymbol{x})$ at the $x = (L+1)/2$ slice with monopole charge $n = -2$ is plotted. (right panel) The same as the left panel but for the second negative nearest-zero mode $A_2(\boldsymbol{x})$.

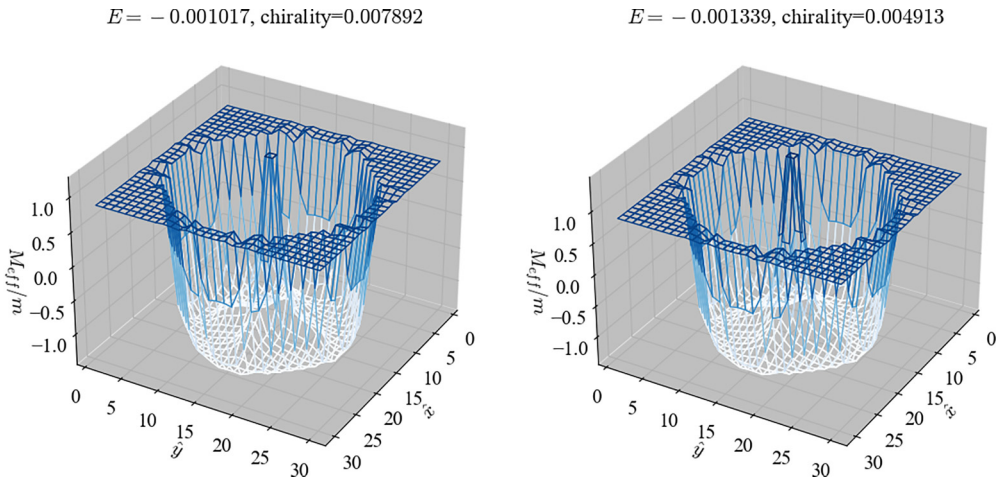

FIG. 6. The local effective mass (defined in the main text) normalized by m_0 at the $z = (L+1)/2$ slice for the negative nearest-zero mode ϕ_1. The results for the magnetic charge $n = +1$ (left panel) and $n = -2$ (right panel) are plotted. The data are shown with gradation to make explicit the two regions of normal phase with $m_{\text{eff}}/m_0 \sim +1$ in dark mesh and the one for topological phase with $m_{\text{eff}}/m_0 \sim -1$ in light mesh.

of the $2|n|$ nearest-zero modes with magnetic charge $n = 1$ (left panel) and $n = -2$ (right panel). They all show a stable plateau in the middle range $4 < r < 9 = 3r_0/4$ at $C_k(r) \sim 1/2$. Therefore, we can conclude that under the half filling condition, the monopole gains $|n|/2$ electric charge capturing the half of the occupied $|n|$ zero-mode states of the electron.

VI. EFFECTIVE THEORY REVISITED AND SIMULATION WITH NONINTEGRAL MAGNETIC CHARGE

A. Reinterpretation of the effective action description

The above analysis suggests an interesting reinterpretation of the original argument in the effective Lagrangian of the Maxwell theory in Sec. II. When we integrate out the electron fields in the presence of a single monopole, the effective action contains a position-dependent θ term:

$$S_{\text{top.}} = \frac{1}{32\pi^2}\int d^4x\theta(r)F_{\mu\nu}\tilde{F}^{\mu\nu}, \tag{93}$$

$$\theta(r) = \pi\Theta(r-r_2)\Theta(r_0-r) = \begin{cases}\pi & \text{for } r_2 < r < r_0\\ 0 & \text{otherwise,}\end{cases} \tag{94}$$

where $\Theta(r)$ denotes the step function. As in the previous section, r_2 is the size of the positive mass region around the monopole, while r_0 is the location of the surface when the topological insulator is spherical.[13]

Then the Maxwell equation is modified as

$$\partial_\mu F^{\mu\nu} = -\frac{1}{8\pi^2}\partial_\mu[\theta(r)\tilde{F}^{\mu\nu}]. \tag{95}$$

When we evaluate the volume integral inside the topological insulator $r < r_0$, we have

$$\begin{aligned} q_e &= \int_{r<r_0} d^3x\nabla\cdot\boldsymbol{E} = -\frac{\theta}{4\pi^2}\int_{r<r_0} d^3x\nabla\theta(r)\cdot\boldsymbol{B}\\ &= -\frac{\theta}{4\pi^2}\int_{r<r_0} d^3x\pi\delta(r-r_1)\boldsymbol{e}_r\cdot\boldsymbol{B}\\ &= -\frac{1}{2}. \end{aligned} \tag{96}$$

[13]The shape of the outer surface is not important here.

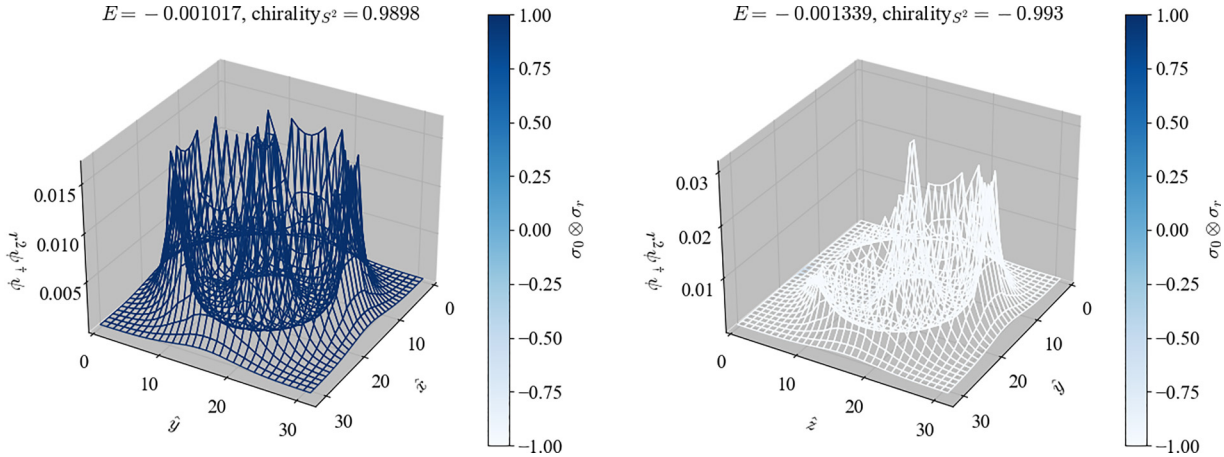

FIG. 7. The same plot as the left panel of Figs. 4 and 5 but with the gradation indicating the two-dimensional chirality $1 \otimes \sigma_r$ locally measured.

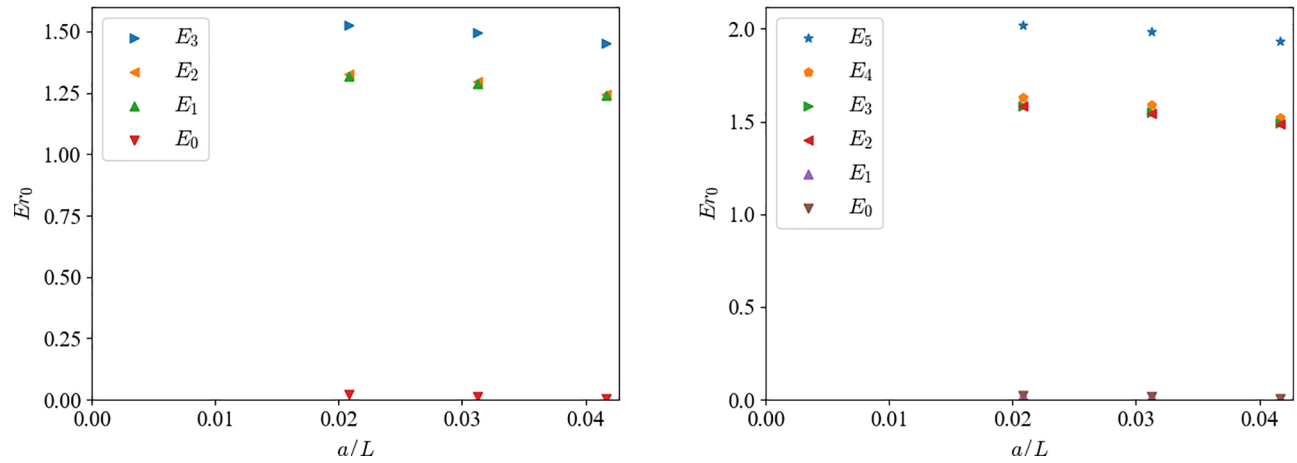

FIG. 8. The lattice cutoff a/L dependence of the negative nearest-zero eigenvalues. The results for $n = 1$ (left panel) and those for $n = -2$ (right panel) are shown.

The result is consistent with Eq. (5) but it does not require $\nabla \cdot \boldsymbol{B} \neq 0$, provided contribution from the Dirac string can be safely neglected.

The same argument applies to the case with a two-dimensional vortex with $\alpha = 1/2$. The effective action after integrating out the fermion can be treated as the Chern-Simons action with a position-dependent level $k(r) = \Theta(r - r_1)\Theta(r_0 - r)$, and the Maxwell equation becomes

$$\partial_\mu F^{\mu\nu} = -\frac{1}{8\pi^2}\partial_\mu[k(r)\epsilon^{\mu\nu\rho}A_\rho]. \tag{97}$$

The electric charge around the vortex

$$\begin{aligned} q_e &= \int_{r<r_0} d^2x \nabla \cdot \boldsymbol{E} = -\frac{1}{2\pi}\int_{r<r_0} d^2x \partial_r k(r) A_\theta \\ &= -\frac{1}{2\pi}\int_{r<r_0} d^2x \delta(r - r_1)A_\theta = -\frac{r_1}{2\pi}\int_0^{2\pi} d\theta A_\theta \\ &= -\frac{1}{2}, \end{aligned} \tag{98}$$

is again consistent with Eq. (7) but it does not require any singularity of the gauge field.

B. Nonintegral magnetic charge

Knowing the fact that the singularity of the gauge field: $\nabla \cdot \boldsymbol{B} \neq 0$ is not necessarily required to gain the electric charge, we would like to propose an interesting (thought) experiment that may allow us to observe the Witten effect without true monopoles.

Suppose we have a thin solenoid whose radius is comparable to the crystal spacing of a topological insulator. Inserting one end of the solenoid inside the topological insulator while the other end is put outside, we can mimic the monopole-antimonopole system with a fine-tuned electric current around the solenoid. The solenoid represents the Dirac string.

This experiment can be simulated with our lattice setup continuously varying the value of n from 0 to 1. The n dependence of the amplitude weighted by r^2 of the positive nearest zero mode at the slice $x = (L + 1)/2$ is presented in Fig. 10.

At $n = 0$ the energy eigenvalue is nonzero, $E \approx 0.08$, and the amplitude is uniformly distributed around the sphere of radius $r = r_0$. Increasing n, a part of the wave function is gradually swallowed into the topological insulator from bottom of the sphere. At $n = 0.5$, the amplitude along the Dirac string reaches maximum, and the energy eigenvalue is reduced to

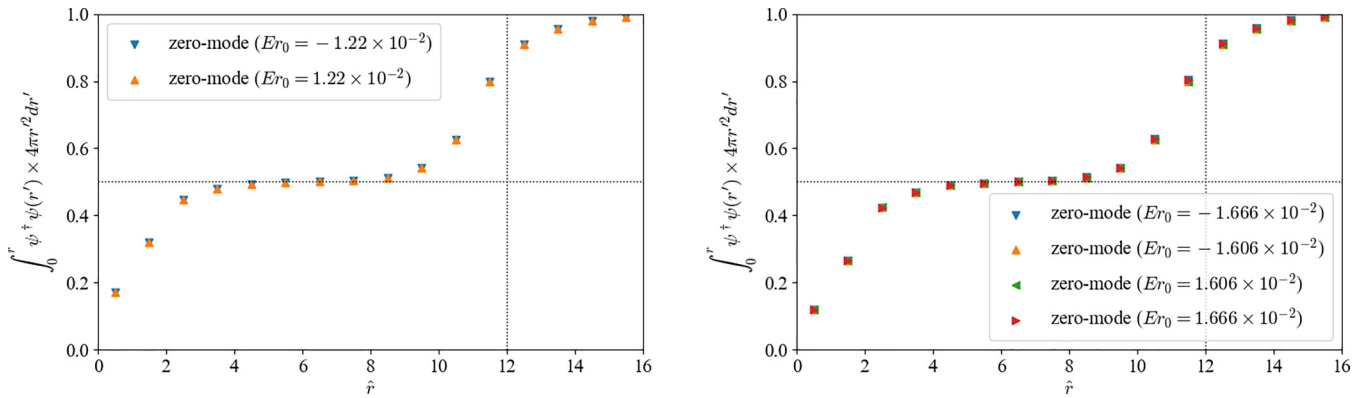

FIG. 9. Cumulative eigenfunction distribution of the nearest-zero modes inside r, which gives an estimate for the electric charge captured by the monopole. The case with $n = 1$ (left panel) and that with $n = -2$ (right panel) are plotted. At $4 < r < 9 = 3r_0/4$ we observe a stable plateau at $1/2$.

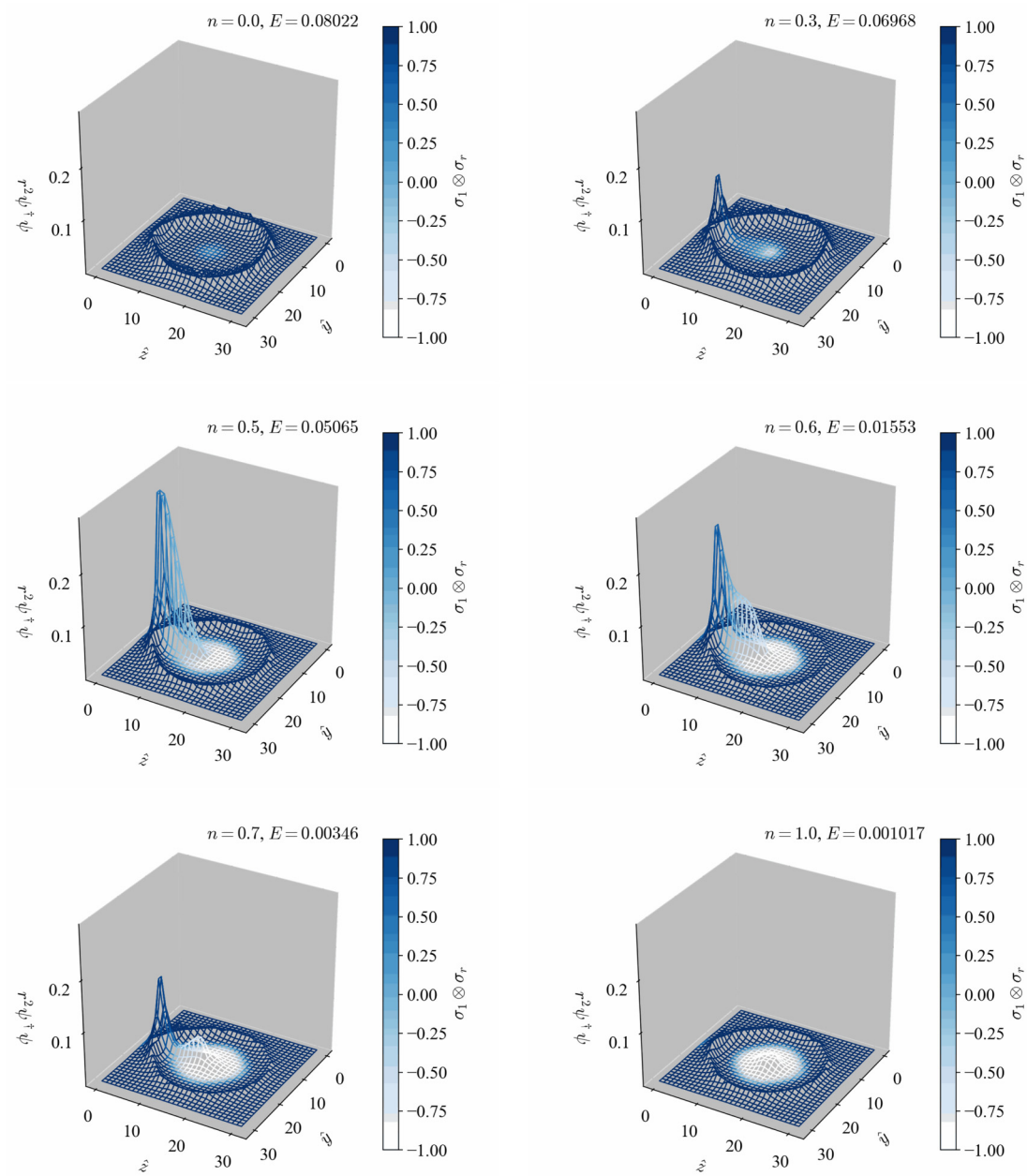

FIG. 10. The amplitude (weighted by r^2) of the nearest-zero eigenfunction of H_W at the slice $x = (L + 1)/2$. By a continuous deformation of the monopole charge from $n = 0$ to $n = 1$, half of the wave function goes into the vicinity of the monopole through the Dirac string.

$E \approx 0.05$. For larger $n > 0.5$ the wave function is separated into two; one half is attracted by the monopole, while the other half stays at the original domain wall. At $n = 1$, the energy is reduced to almost zero.

In this process let us focus on a two-dimensional slice at a fixed z coordinate along the Dirac string. The slice corresponds to the two-dimensional topological insulator with a vortex discussed in Sec. III. Note that the flux of the vortex is equal to the monopole charge $\alpha = n$. In Sec. III, we have learned that the energy of the electron is minimized at $\alpha = 1/2$ where the Aharonov–Bohm (AB) effect is maximized and the wave function is localized at the vortex. This explains why the amplitude of the electron at $n = 0.5$ is attracted by the Dirac string. At $\alpha = n = 1$, the AB effect becomes zero and the Dirac string cannot attract the electron field any longer, while the binding force from the monopole is maximized to capture the half of the electron field amplitude.

For $1 < n < 2$ a similar cycle starts on the second nearest zero mode. The same continues for $n > 3$ and the charge proportional to $|n|/2$ is, thus, pumped from the outer domain wall to the monopole.

It is also interesting to trace the topology change of the domain wall shown in Fig. 11. Increasing n from zero to $1/2$, the mass shift along the Dirac string becomes large, making a bridge of normal insulators connecting the $r > r_0$ region and the location of the monopole. By the time the monopole charge reaches $n = 1$, the Dirac string neighbor becomes back to the topological insulator again, and the bridge is disconnected to end up with two spherical domain walls: one at the original $r = r_0$ and the other at the vicinity of the monopole.

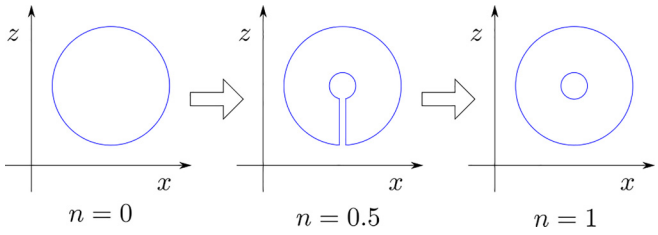

FIG. 11. Schematic image of topology change of the domain wall. One spherical domain wall at $n = 0$ is extended via the Dirac string into the location of the monopole at $n \approx 0.5$ and is separated into two domain walls at $n = 1$.

VII. SUMMARY AND DISCUSSION

In this work, we have investigated the microscopic mechanism how a vortex or monopole in topological insulators becomes a dyon gaining a half-integral electric charge. In our analysis we have added the Wilson term to the Dirac equation, compared with which the sign of the electron mass has a physical meaning. We have also smeared the singularity of the gauge field in a finite region of radius r_1, which makes our computations always UV finite. In this set up, we have obtained the (near) zero-mode solutions both analytically in continuum and numerically on a lattice.

The key finding in this work is dynamical creation of a domain wall around the monopole or vortex. We have confirmed that the local mass shift from the Wilson term is of size $1/r_1$ that is positive. This mass shift is strong enough to make a small island of a normal insulator around the monopole or vortex. The edge-localized modes on the domain wall can be identified as the origin of the electric charge captured by the monopole or vortex. In the $r_1 = 0$ limit with a quantized magnetic charge $q_m = 1/2 \bmod \mathbb{Z}/2$ or flux $\alpha = 1 \bmod \mathbb{Z}$, only the chiral modes survive with energy zero.

The fact that the created domain wall is not a point-like singularity but a codimension-one sphere having the same dimensions that the outer surface of the target topological insulator has, makes the topological meaning of the zero modes clearer. In mathematics, the two manifolds of the same dimension are cobordant if their disjoint union is the boundary of a compact manifold one dimension higher. In our physics target, it is clear that the dynamically created small domain wall at $r = r_1$ around the vortex or the one at $r = r_2 \sim 1/M_{\rm PV}$ around the monopole, and the surface at $r = r_0$ of the topological insulator are cobordant since they are the boundaries of the same topological insulator having a negative mass. We have also identified the number of the chiral zero modes as the Atiyah-Singer or mod-two Atiyah-Singer index, which is a cobordism invariant: they must appear in pairs on the domain wall $r = r_1$ or r_2 and on the one at $r = r_0$.

For each set of the two zero modes paired by the cobordism, we have computed their mixing amplitude both analytically and numerically. Due to the chiral symmetry of the total system, at whatever large distance r_0, the mixing is always maximum: 50% vs 50%, which explains why the electric charge expectation value around the monopole or vortex is $1/2$ in the half filling state, where only one of the two split near zero modes is occupied.

From our microscopic analysis we have suggested an interesting reinterpretation of the effective theory approach. After integrating out the massive electron fields, the system contains a defect not in the gauge field but in the θ parameter or the level k of the Chern-Simons action. The modified Maxwell equation still gives the same half-integral electric charge but does not require any singularity of the gauge field, since the monopole or vortex is located in the trivial $\theta = 0$ or $k = 0$ region.

This implies that the Witten effect can be observed in our laboratory even without true monopoles. We have simulated a thin solenoid, which corresponds to the Dirac string, with one end inserted into a topological insulator and the other end outside. Increasing the magnetic flux of the solenoid, we have observed that a bridge of normal insulators along the solenoid appears between the surface and the monopole. Then a pair of the near-zero edge modes on the surface gradually crosses the bridge towards the monopole, decreasing its energy to zero. By the time the magnetic flux reaches that of a unit magnetic monopole, half of the wave function arrives at the monopole, and the bridge disappears. In this process, a single domain wall sphere is separated into two, to populate a pair of chiral zero modes.

It is interesting to investigate how stable our results are against perturbation of the Hamiltonian due to impurities or external interference. While in the original discussion in Ref. [5] the half integral charge depends only on the T-symmetric value of $\theta = \pi/2$, our analysis has relied on an additional chiral symmetry with $\bar{\gamma}$ to show topological stability of the zero modes. It is a good challenge to examine if breaking of the chiral symmetry while keeping the T symmetry changes the results.

In the tight-binding models, there may be higher-order terms than the Wilson term, which can change the sign of the effective mass back to negative in a region smaller than the radius r_1. Even in such a case, the cobordism invariance of the AS index will protect the number of net-zero modes including the chirality to be the same as the surface zero modes.

ACKNOWLEDGMENTS

We thank Mikio Furuta, Masahiro Hotta, Takuto Kawakami, Tsunehide Kuroki, Okuto Morikawa, Tetsuya Onogi, Shigeki Sugimoto, Kazuki Yamamoto, Masahito Yamazaki, and Ryo Yokokura for useful discussions. The work of S.A. was supported by JST SPRING, Grant No. JPMJSP2138. The work of H.F. and N.K. was supported by JSPS KAKENHI Grant No. JP22H01219. The work of M.K. was supported by JSPS KAKENHI Grants No. JP21H05236, No. JP21H05232, No. JP20H01840, and No. JP20H00127, and the work by JST CREST was supported by Grant No. JPMJCR20T3, Japan.

[1] P. A. M. Dirac, Quantised singularities in the electromagnetic field,, Proc. R. Soc. London, Ser. A **133**, 60 (1931).

[2] G.'t Hooft, Magnetic monopoles in unified gauge theories, Nucl. Phys. B **79**, 276 (1974).

[3] A. M. Polyakov, Particle spectrum in quantum field theory, JETP Lett. **20**, 194 (1974).

[4] A. H. Guth, The inflationary universe: A possible solution to the horizon and flatness problems, Phys. Rev. D: Part. Fields **23**, 347 (1981).

[5] E. Witten, Dyons of charge $e\theta/2\pi$, Phys. Lett. B **86**, 283 (1979).

[6] C. G. Callan, Jr., Disappearing dyons, Phys. Rev. D: Part. Fields **25**, 2141 (1982).

[7] C. G. Callan, Jr., Dyon-fermion dynamics, Phys. Rev. D: Part. Fields **26**, 2058 (1982).

[8] V. A. Rubakov, Adler-Bell-Jackiw anomaly and fermion number breaking in the presence of a magnetic monopole, Nucl. Phys. B **203**, 311 (1982).

[9] J. A. Harvey, Magnetic monopoles, duality and supersymmetry, in ICTP Summer School in High-Energy Physics and Cosmology, arXiv:hep-th/9603086.

[10] L. Alvarez-Gaume and F. Zamora, Duality in quantum field theory and string theory, AIP Conf. Proc. **423**, 46 (1998).

[11] M. Pretko, Higher-spin Witten effect and two-dimensional fracton phases, Phys. Rev. B **96**, 125151 (2017).

[12] N. Yamamoto, Magnetic monopoles and fermion number violation in chiral matter, arXiv:2005.05028.

[13] M. Abe, O. Morikawa, and H. Suzuki, Fractional topological charge in lattice Abelian gauge theory, Prog. Theor. Exp. Phys. **2023**, 023B03 (2023).

[14] P. Sikivie, On the interaction of magnetic monopoles with axionic domain walls, Phys. Lett. B **137**, 353 (1984).

[15] Y. Hidaka, M. Nitta, and R. Yokokura, Higher-form symmetries and 3-group in axion electrodynamics, Phys. Lett. B **808**, 135672 (2020).

[16] H. Fukuda and K. Yonekura, Witten effect, anomaly inflow, and charge teleportation, J. High Energy Phys. 01 (2021) 119.

[17] A. Sekine and K. Nomura, Axion electrodynamics in topological materials, J. Appl. Phys. **129**, 141101 (2021).

[18] P. Agrawal, K. V. Berghaus, J. Fan, A. Hook, G. Marques-Tavares, and T. Rudelius, Some open questions in axion theory, in 2022 Snowmass Summer Study, arXiv:2203.08026.

[19] Y. Hamada, R. Kitano, R. Matsudo, and K. Mukaida, Understanding anomalous particle production in massless QED via time-varying θ angle, J. High Energy Phys. 09 (2022) 218.

[20] Y. Choi, H. T. Lam, and S.-H. Shao, Non-invertible Gauss law and axions, arXiv:2212.04499.

[21] L. Fu, C. L. Kane, and E. J. Mele, Topological insulators in three dimensions, Phys. Rev. Lett. **98**, 106803 (2007).

[22] L. Fu and C. L. Kane, Topological insulators with inversion symmetry, Phys. Rev. B **76**, 045302 (2007).

[23] J. E. Moore and L. Balents, Topological invariants of time-reversal-invariant band structures, Phys. Rev. B **75**, 121306(R) (2007).

[24] X.-L. Qi, T. L. Hughes, and S.-C. Zhang, Topological field theory of time-reversal invariant insulators, Phys. Rev. B **78**, 195424 (2008).

[25] A. P. Schnyder, S. Ryu, A. Furusaki, and A. W. W. Ludwig, Classification of topological insulators and superconductors in three spatial dimensions, Phys. Rev. B **78**, 195125 (2008).

[26] R. Roy, Topological phases and the quantum spin Hall effect in three dimensions, Phys. Rev. B **79**, 195322 (2009).

[27] T. Sasaki, E. Imai, and I. Kanazawa, Witten effect and fractional electric charge on the domain wall between topological insulators and spin ice compounds, J. Phys.: Conf. Ser. **568**, 052029 (2014).

[28] H.-G. Zirnstein and B. Rosenow, Topological magnetoelectric effect: Nonlinear time-reversal-symmetric response, Witten effect, and half-integer quantum Hall effect, Phys. Status Solidi B **257**, 1900698 (2020).

[29] C.-Y. Hou, C. Chamon, and C. Mudry, Electron fractionalization in two-dimensional graphenelike structures, Phys. Rev. Lett. **98**, 186809 (2007).

[30] A. Mesaros, R.-J. Slager, J. Zaanen, and V. Juricic, Zero-energy states bound to a magnetic π-flux vortex in a two-dimensional topological insulator, Nucl. Phys. B **867**, 977 (2013).

[31] E. Lee, A. Furusaki, and B.-J. Yang, Fractional charge bound to a vortex in two-dimensional topological crystalline insulators, Phys. Rev. B **101**, 241109(R) (2020).

[32] B. Messias de Resende, F. C. de Lima, R. H. Miwa, E. Vernek, and G. J. Ferreira, Confinement and fermion doubling problem in Dirac-like Hamiltonians, Phys. Rev. B **96**, 161113(R) (2017).

[33] Y. Kazama, C. N. Yang, and A. S. Goldhaber, Scattering of a Dirac particle with charge Ze by a fixed magnetic monopole, Phys. Rev. D: Part. Fields **15**, 2287 (1977).

[34] A. S. Goldhaber, Dirac particle in a magnetic field: Symmetries and their breaking by monopole singularities, Phys. Rev. D: Part. Fields **16**, 1815 (1977).

[35] C. J. Callias, Spectra of fermions in monopole fields: Exactly soluble models, Phys. Rev. D: Part. Fields **16**, 3068 (1977).

[36] H. Yamagishi, Fermion-monopole system reexamined, Phys. Rev. D: Part. Fields **27**, 2383 (1983).

[37] B. Grossman, Does a dyon leak? Phys. Rev. Lett. **50**, 464 (1983).

[38] H. Yamagishi, Fermion-monopole system reexamined. II, Phys. Rev. D: Part. Fields **28**, 977 (1983).

[39] Y.-Y. Zhao and S.-Q. Shen, A magnetic monopole in topological insulator: exact solution, arXiv:1208.3027.

[40] A. C. Tyner and P. Goswami, Part II: Witten effect and $\mathbb{Z}$-classification of axion angle $\theta = n\pi$, arXiv:2206.10636.

[41] R. Jackiw and C. Rebbi, Solitons with fermion number 1/2, Phys. Rev. D: Part. Fields **13**, 3398 (1976).

[42] C. G. Callan Jr. and J. Harvey, Anomalies and fermion zero modes on strings and domain walls, Nucl. Phys. B **250**, 427 (1985).

[43] D. B. Kaplan, A method for simulating chiral fermions on the lattice, Phys. Lett. B **288**, 342 (1992).

[44] Y. Shamir, Chiral fermions from lattice boundaries, Nucl. Phys. B **406**, 90 (1993).

[45] V. Furman and Y. Shamir, Axial symmetries in lattice QCD with Kaplan fermions, Nucl. Phys. B **439**, 54 (1995).

[46] K.-I. Imura and Y. Takane, Protection of the surface states in topological insulators: Berry phase perspective, Phys. Rev. B **87**, 205409 (2013).

[47] S. Aoki and H. Fukaya, Curved domain-wall fermions, Prog. Theor. Exp. Phys. **2022**, 063B04 (2022).

[48] S. Aoki and H. Fukaya, Curved domain-wall fermion and its anomaly inflow, Prog. Theor. Exp. Phys. **2023**, 033B05 (2023).

[49] M. F. Atiyah and I. M. Singer, The index of elliptic operators on compact manifolds, Bull. Am. Math. Soc. **69**, 422 (1963).

[50] M. F. Atiyah and I. M. Singer, The index of elliptic operators: I, Ann. Math. **87**, 484 (1968).

[51] M. F. Atiyah and I. M. Singer, The index of elliptic operators: V, Ann. Math. **93**, 139 (1971).

[52] G. Rosenberg and M. Franz, Witten effect in a crystalline topological insulator, Phys. Rev. B **82**, 035105 (2010).

[53] Y. Hatsugai, Chern number and edge states in the integer quantum hall effect, Phys. Rev. Lett. **71**, 3697 (1993).

[54] Y. Hatsugai, Edge states in the integer quantum Hall effect and the Riemann surface of the Bloch function, Phys. Rev. B **48**, 11851 (1993).

[55] V. R. Khalilov, Bound states of massive fermions in Aharonov-Bohm-like fields, Eur. Phys. J. C **74**, 2708 (2014).